A Simple Transformer-Based Resonator Architecture for Low Phase Noise LC Oscillators

By

Olumuyiwa Temitope Ogunnika

B.E. Electrical Engineering
The City College of the City University of New York, 2001

Submitted to the Department of Electrical Engineering and Computer Science
in partial fulfillment of the requirements for the degree of

Master of Science in Electrical Engineering and Computer Science
at the
MASSACHUSETTS INSTITUTE OF TECHNOLOGY
[February 2004]
October 2003

Author.....
Department of Electrical Engineering
and Computer Science
October 2, 2003

Certified by.....
Michael H. Perrott
Assistant Professor of Electrical Engineering and Computer Science
Thesis Supervisor

Accepted by.....
Arthur C. Smith
Chairman, Department Committee on Graduate Theses

A Simple Transformer-Based Resonator Architecture for Low Phase Noise LC Oscillators

By

Olumuyiwa Temitope Ogunnika

Submitted to the Department of Electrical Engineering and Computer Science
On October 2, 2003, in partial fulfillment of the
requirements for the degree of
Master of Science in Electrical Engineering and Computer Science
at the
MASSACHUSETTS INSTITUTE OF TECHNOLOGY

Abstract

This thesis investigates the use of a simple transformer-coupled resonator to increase the loaded Q of a LC resonant tank. The windings of the integrated transformer replace the simple inductors as the inductive elements of the resonator. The resonator topology considered in this project is a simpler alternative to another proposed by Straayer et al [5] because it just requires a single varactor. A prime objective of this project is to prove that a transformer-coupled resonator which is simpler than that proposed by Straayer in [5] produces the same reduction in phase noise. The use of this type of resonator topology is a valuable technique which can be employed by RF engineers to reduce the phase noise generated by oscillators in high speed RF systems. Such techniques which increase the loaded Q of the resonator are very useful in practice because of the inverse squared relationship between resonator Q and the phase noise in the output signals of LC oscillators.

The important aspect of this technique is that magnetic coupling between the windings of an integrated transformer increases their effective inductance while leaving their series resistance relatively unchanged. As a result, the Q of these inductive elements is increased and the phase noise generated by the oscillator is reduced. SpectreRF simulations of an LC oscillator with a center frequency of 5GHz were used to verify the performance of the proposed transformer-coupled resonator.

Thesis Supervisor: Michael H. Perrott
Title: Assistant Professor of Electrical Engineering

Acknowledgement

I thank God for giving me the privilege of completing my Masters degree at a prestigious institution such as MIT. Through the many months during which I have been working on this project, He has been my source of strength and encouragement. I owe my life and health to Him and I will be forever grateful for His kindness and mercy. I thank Him for the salvation He has given me through my Lord and Savior Jesus Christ.

To my parents, Prof. Olu Ogunnika and Mrs. Olabisi Ogunnika: Thank you for loving, encouraging and believing in me all these years. Words cannot express how grateful I am for all you have done for me. You have sacrificed so much for me over the last 25 years and I pray that I can continue to make you proud.

To my siblings, Femi, Toyin and Seun: Thank you for being the best siblings a brother can have! My fondest memories of growing up with you will always be with me. You can always count on me for love and support in all your future endeavors.

I'd like to thank my advisor, Prof. Michael Perrott for helping me to complete this project. Your guidance has been essential in helping me to understand many of the concepts I encountered over the duration of this thesis work. I am very grateful for all the advice you have given me concerning the development of research skills necessary to succeed in graduate school.

My lab mates Scott Meninger, Charlotte Lau, Shawn Kuo, and Belal Helal have been great people to know and associate with. My thanks to Scott Meninger who helped me immensely in analyzing many of the technical issues I had to deal with. We spent countless hours pouring over circuit schematics and transformer structures for which I still owe him a couple of beers!

Contents

Chapter 1

Introduction

1.1 Motivation

In the world today, the economies of all countries are intricately interconnected and interdependent in global trade and exchange of information. This would not be possible without the efficient transmission of information by various means including wireless communication systems. The need to transmit more information in a reliable and efficient manner has led to a significant increase in the demand for more efficient RF systems operating at higher frequencies. The limited frequency bands available for cellular, satellite and radio communication systems make it essential that these frequency bands are efficiently utilized. In many communication systems, the efficacy of utilization is dependent on how many different channels can operate within a given frequency band without undue interference. The problem with wireless systems in general is that they are plagued with interference and signal degradation in the form of phase noise.

Phase noise is very detrimental to the acceptable performance of RF systems for a number of reasons. An RF system which produces an output signal with too much phase noise will produce unwanted signals can act as interferers to other RF systems which operate at relatively close frequencies. This interference can significantly degrade the signal to noise ratio of these systems and reduce the reliability and accuracy of the information transferred. As a result, the Federal Communications Commission (FCC) has laid down very strict guidelines for the output spectrum of wireless communication

systems. These restrictions have a direct impact on the magnitude of phase noise which is acceptable at a particular offset from the carrier frequency of these RF systems. These problems make the reduction of phase noise in RF systems a very active area of research for RF engineers.

Most RF systems contain an oscillator which is used to generate the periodic output signal that is modulated with the information to be transmitted. Unfortunately, these oscillators are a dominant source of phase noise and signal degradation in these systems. Thus, the author believes it is very important to investigate methodologies and techniques that can be used to reduce the phase noise introduced into RF systems by oscillators. A good understanding of the techniques used to reduce the phase noise generated by oscillators will go a long way in making current wireless communication systems more efficient and economical. The breaking of new frontiers in the continuous integration of the different economies in our world today would then be assured.

The goal of this project is to show that the reduction in phase noise obtained by the resonator proposed by Straayer et al in [5] can also be achieved with the simpler transformer-coupled resonator architecture discussed in Chapter 5. It involves replacing the simple inductor used in the resonator by an integrated transformer. Keeping the oscillator's architecture as simple as possible is always desirable because it reduces the problems created by the inevitable mismatch in the properties of integrated devices on the same silicon substrate.

1.2 Outline of Thesis

Chapter 1 gives a brief overview of the motivation and goal of this thesis project. Chapter 2 discusses the modeling and characteristics of oscillators used in RF systems. This serves as a background for the understanding of the discussion about LC resonators in Chapter 5. Chapter 3 introduces the concept of phase noise and describes a number of phase noise models used to analyze the phase noise in oscillators. Chapter 4 discusses a number of methods used to reduce phase noise in oscillators. The technique which involves the increase of the resonator Q by means of a transformer-coupled architecture will be the focus of this project. Chapter 5 looks into inductor structures that can be used in oscillators to improve their phase noise performance. In particular, the reduction in the phase noise of an oscillator by replacing the inductors in the resonator with an integrated transformer is discussed. A comparison will be made between the expected improvements in phase noise performance obtained from hand calculations and simulation results from SpectreRF. In addition, the chapter proves that this simpler transformer-coupled resonator topology has the same phase noise performance as an alternative topology proposed by Straayer et al in [5]. Chapter 6 describes the modeling and design of the inductor and transformer which are most critical components of an LC resonator. This chapter is very important because of the traditionally low Q-factors of these passive elements in standard VLSI processes. Chapter 7 analyzes the effects of a mismatch in the inductances of the transformer windings on the performance of the transformer-based oscillator topology in Chapter 5. This analysis is essential because it is practically impossible to create two identical devices or components in any silicon process. This thesis concludes with Chapter 8 which gives a summary of the important results obtained in this project.

Appendix A goes into more detail about the alternative transformer-coupled resonator proposed by Straayer et al [5].

1.3 Summary

This chapter has provided the motivation and main objective of this thesis project. The fact that the design of low phase noise LC oscillators is essential for the fabrication of high speed, high performance RF systems was emphasized. The goal of this project which is to prove that a simpler transformer-based architecture produces the same phase noise reduction as the architecture in [5] was also stated. The next chapter will give a brief introduction to oscillators which is important in understanding the subject matter of the remaining chapters.

Chapter 2

Oscillators

This chapter presents a brief introduction to the concept of oscillators in RF systems. It is necessary for the reader to have a good understanding of the mode of operation of oscillators before the concepts of phase noise and increase in the Q-factor of LC resonators can be introduced. The two general models used to analyze the operation of an oscillator and a number of practical oscillators common in the literature will be discussed. A particular group of oscillators called LC resonator oscillators are particularly suited to the transformer-coupled resonator approach of reducing the phase noise in oscillators. Thus, these oscillators will be discussed so that the concepts and explanations of why an oscillator that employs a transformer-coupled resonator shows a reduced magnitude of phase noise in its output signal can be understood.

2.1 What is an Oscillator?

An oscillator is a system which generates a periodic output signal. Voltage controlled oscillators (VCO) are oscillators in which the output frequency is proportional to an applied external voltage. Thus, VCOs are found in electronic systems which require a source of variable frequency used for frequency synthesis, clock and data recovery and other applications. These circuits are particularly important in PLL systems used for clock generation and synchronization. Oscillators are found in many audio and RF sys-

tems including but not limited to audio/music synthesizers, radio transmitters and receivers, etcetera.

Oscillators must have some sort of self-sustaining mechanism to ensure that they continue to generate these periodic signals for an indefinite period of time. The basic operation of all oscillators involves the positive feedback of the output of the oscillator to its input. Thus, the periodic signal sustains and regenerates itself from one cycle to the other.

Quartz crystals are a popular means of building oscillators. When a direct current is applied to these crystals, they vibrate at a frequency that depends on their thickness, and on the manner in which they were cut from the original mineral rock. Quartz crystals produce periodic signals with little phase noise and relatively small extraneous signal components. But they occur at relatively low frequencies in the MHz range which are not high enough for RF applications. Thus, oscillators employing a combination of storage elements such as inductors and capacitors are commonly used in high speed RF systems.

2.2 Oscillator Models

Oscillators are usually analyzed based on two equivalent models: either as a two port system or a one-port system made up of two interconnected sub-systems. The two port model shown in Figure 2-1 shows a frequency selective network or resonator in the feedback loop. The H(s) block is the feed-forward gain block which is simply an amplifier; the G(s) block is the feedback block which also stabilizes or selects the frequency of

the oscillator. The loop gain of this system is G(s)H(s) and this term is used in the Barkhausen criteria discussed in the next paragraph.

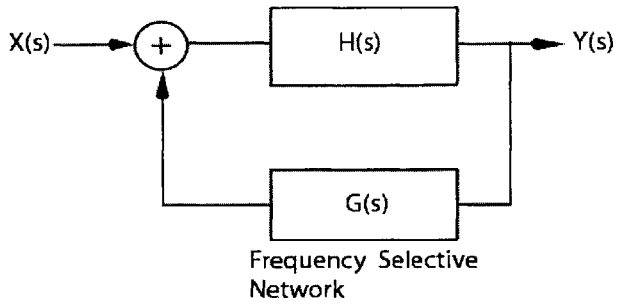

Figure 2-1: Two port oscillator model

The transfer function of the system is given by,

$$\frac{Y(s)}{X(s)} = \frac{G(s)H(s)}{1-G(s)H(s)}$$

In order for this system to produce a sustainable oscillation with a frequency, $s_0=j\omega_0$, the Barkhausen criteria must be satisfied: (1) The closed loop gain must be equal to unity at the frequency of oscillation, i.e. $G(s_0)H(s_0) = +1$; (2) The total phase shift around the loop must be equal to 0° for positive feedback and 180° for negative feedback. These criteria show that any feedback system can oscillate if the closed loop gain and phase shift from input to output are suitably chosen.

In an LC oscillator, the frequency selective network or resonator is composed of an inductor and capacitor which are introduced to select and stabilize the oscillator's output frequency. In voltage controlled oscillators (VCOs), the capacitor takes the form of a varactor whose capacitance can be varied to change the center frequency of the oscillator. The capacitance of the varactor is varied by means of an externally applied bias voltage. This property is essential in applications such as phase locked loops which require the oscillator to operate over a given range of frequencies. The block with transfer function,

H(s), is usually a transistor circuit whose purpose is to provide sufficient gain so that a constant periodic output signal can be sustained. This block can be a single transistor like in the simple Colpitts oscillator of Figure 2-2a or it can be made up of two or more transistors like the differential oscillator of Figure 2-2b.

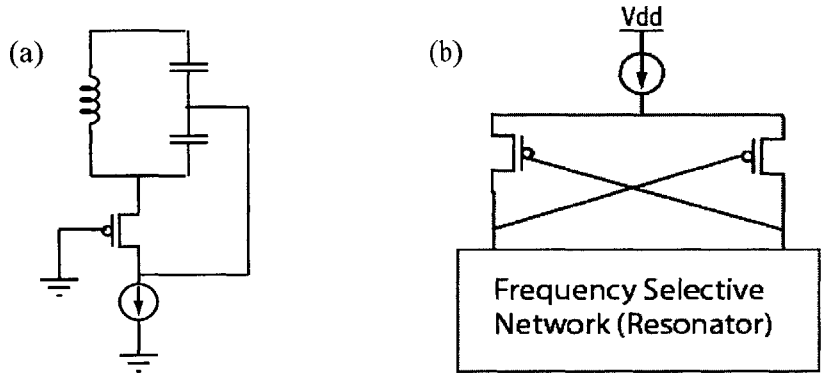

Figure 2-2: Two feedback oscillator topologies: (a) Colpitts oscillator, (b) Differential push-pull oscillator.

Alternatively, the one port model (Figure 2-3) can be used to gain more insight and understanding of the operation of oscillators. This model describes the oscillator as composed of two one-port networks connected together. These networks are the active device network and the frequency selective network or resonator. A constant periodic output signal is obtained by the exchange of energy between the inductors and capacitors in the resonator. But in any practical circuit, these passive components have parasitic resistances associated with them. Therefore, the resonator is unable to sustain an output signal of constant amplitude all by itself because energy is lost every cycle in these parasitic resistances. Therefore, the active device network is introduced to replenish the energy lost per cycle.

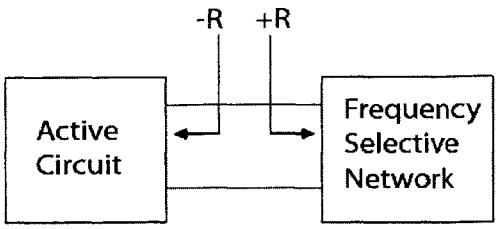

Figure 2-3: One-port model of oscillator

A very useful way of understanding the operation of an oscillator is to consider the one-port model in Figure 2-3 at resonance. The frequency selective tank can be expressed or approximated by a simple parallel RLC circuit with equivalent parallel resistance, R. This is the resistance responsible for the loss in stored energy per cycle. The active circuit compensates for this loss by providing a negative resistance, -R, of equal amplitude to the equivalent parallel resistance of the resonator. Thus, from an operational point of view, the resistance of the resonator is cancelled out and it appears as a lossless network. The oscillator can now sustain an output signal of constant amplitude.

Another important point to address is the startup of LC oscillators. To ensure startup, the closed loop gain of the oscillator circuit is set to a value greater than unity. This ensures that the noise inherently present in the oscillator is amplified until a signal of suitable large amplitude is obtained. The magnitude of the output signal does not grow out of control because of the amplitude limiting mechanism present in practical oscillators. These mechanisms are produced by the inherent non-linearity of the transistor devices used in the active circuit network.

2.3 Types of Oscillators

There are a number of criteria by which oscillators can be classified. One such criterion is whether the oscillator possesses a resonator or not. This classification arises from the fact that any amplifier will oscillate if the Barkhausen criteria is satisfied even though it

does not have a resonator. As long as there is sufficient gain at the zero phase frequency, the amplifier circuit will oscillate. In addition, some circuits whose open loop transfer functions exhibit hysteresis may oscillate even when the small signal phase shift appears to be insufficient [11].

2.3.1 Resonatorless Oscillators

This class of voltage controlled oscillators is able to sustain a constant periodic output signal without a resonator. Two common examples of this class of oscillators are the ring oscillator and the multivibrator.

2.3.1.1 Ring Oscillator

When a series of variable delay cells are cascaded with a positive feedback loop connecting the first and last variable delay cell, an output periodic signal will be produced if an odd number of inversions from input to output exist. Suppose the delay of each inverter is D and the number of inverters is N. Then the period of oscillation will be 2DN which is the delay of each delay cell multiplied by twice the number of delay cells.

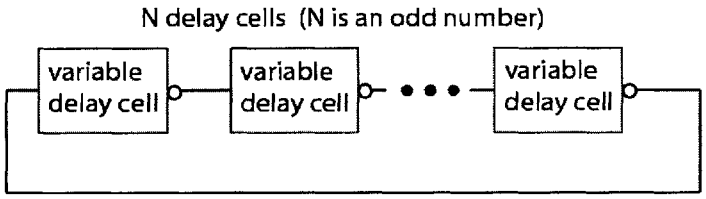

Figure 2-4: Ring Oscillator

This period arises from the fact that the signal has to pass through the inverters twice to get back to its original value because of the odd number of inversions in the feedback loop. The oscillation occurs at a frequency at which the total phase shift is 0° and the loop gain is 1 in accordance with the Barkhausen criteria. Because the delay of

each delay cell can be varied by an external voltage, the period of oscillation of the ring oscillator can be varied as well. This property makes ring oscillators to have a large tuning range which gives them an advantage over other types of oscillators such as LC oscillators. It is worth noting that storage of energy is achieved with the capacitances at the output of the inverters. These capacitances are due to the drain junctions of the output transistors.

2.3.1.2 Relaxation oscillators:

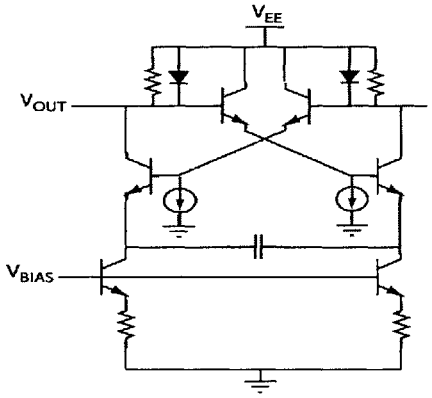

Figure 2-5: Multivibrator

A good example of this type of oscillator is the multivibrator shown in Figure 2-5. This circuit oscillates by continuously charging and discharging a capacitor between two voltage levels. The frequency of oscillation is varied by a voltage controlled current source. By changing the magnitude of the current used to charge the capacitor, the time to charge the capacitor changes as well. Hence, a variation in the output signal frequency is obtained. Multivibrators have the advantage of simplicity and a relatively small number of devices when compared to other resonatorless oscillators.

Resonatorless oscillators are not commonly used in RF design because they contain a relatively large number of active and passive devices in the signal path. Furthermore, these oscillators tend to have very low open loop quality factors. Both of these

properties make resonatorless oscillators to have poor phase noise performance which is unacceptable in modern RF systems which have to satisfy very stringent phase noise specifications. Therefore, the second type of oscillator, which are called resonator oscillators, are more popular in RF systems.

2.3.2 Resonator Oscillators

The most common example of this class of oscillator is the LC oscillator. This oscillator may be designed to produce single-ended, differential or quadrature signals. In an LC oscillator, the periodic signal is generated by means of a network composed of an inductor and a capacitor. A periodic oscillatory output signal is obtained when energy is periodically exchanged between the electric field in the capacitor and the magnetic flux in the inductor.

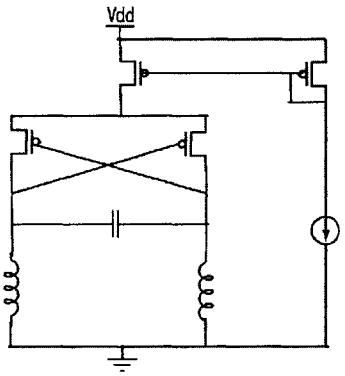

Figure 2-6: Differential LC oscillator

The frequency of oscillation of the differential LC oscillator in Figure 2-6 above can be varied by replacing the capacitor in the resonator with a variable capacitor or varactor. The capacitance of the varactor is changed by varying the magnitude of an external voltage which is applied to the varactor. In standard VLSI processes, the varactor can be the p+/n- well capacitance, the p-n junction capacitance of a reverse biased diode,

or the channel capacitance of a MOSFET with the source and drain shorted. Thus, the oscillation frequency of the oscillator can be "selected" by changing the natural frequency of oscillation of the resonator. It is for this reason that the resonator is also called the frequency selective network.

LC oscillators are the preferred choice for RF systems because of their lower phase noise when compared to relaxation and other resonatorless oscillators. This arises from the fact that LC oscillators require relatively fewer active devices which contribute less device noise. One disadvantage of LC VCOs is that they have a limited tuning range. The varactors which are used to vary the frequency of oscillation of these circuits have a limited range of values over which their capacitance can change. Although the capacitance of a varactor is proportional to the control voltage applied, it cannot increase without bounds because the range of values of the control voltage is limited by the available supply voltage. Some RF circuit designers get around this problem by using a bank of capacitors instead of a single varactor in the resonator. The fixed value capacitors are switched in to tune the VCO over a particular range of frequencies. Thus, the bank of fixed value of capacitors are used for coarse tuning with the varactor is added to fine tune the oscillator to the desired frequency. Caution must be used in the design of these capacitor banks to ensure that the difference in value between successive capacitors is covered by the range of the varactor.

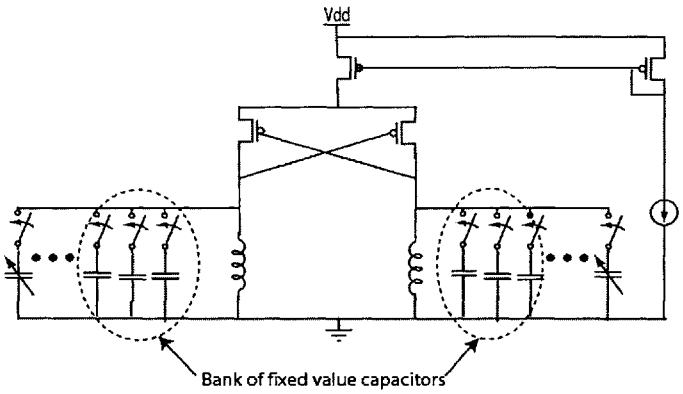

Figure 2-7: LC oscillator with bank of capacitors for coarse tuning.

2.4 Summary

This chapter has provided a brief introduction to the concept of oscillators as a source of periodically varying signals. In particular, the class of oscillators called LC oscillators was discussed in greater detail because they find application in high speed RF systems. The next chapter will introduce the concept of phase noise which is a very important quantity to consider when designing high performance RF systems.

Chapter 3

Phase Noise

3.1 Introduction

Practical oscillators are made up of devices which introduce noise into RF systems. This device noise takes various forms including shot noise, flicker noise, and thermal noise. When this noise is superimposed on the output periodic signal of the oscillator, it leads to a random variation in the output signal's amplitude and frequency. These random variations in the frequency of oscillation can also be regarded as random changes in the position of the zero crossings or phase of the output signal. In this regard, the noise is usually referred to as phase noise. From the equipartition theorem of thermodynamics, half of the device noise in an oscillator is converted to amplitude noise and the other half is converted to phase noise [1]. Since all oscillators have an amplitude control mechanism which prevents the amplitude of oscillation from increasing without bounds, the amplitude noise component is removed by the oscillator and is not significant to the circuit designer. On the other hand, phase noise is a serious concern because it cannot be removed by the oscillator. Thus, it degrades the signal to noise ratio and the integrity of data transmission.

From a frequency domain perspective, the existence of phase noise in oscillators implies that their output signals contain significant energy at other frequencies apart from the desired center frequency. Considering the output spectra shown in Figure 3-1a, significant difference exists between the outputs of ideal and practical oscillators. While an

ideal oscillator has a single spike indicating energy at only one frequency, f_0, a practical oscillator has "skirts" around the center frequency indicating that there is significant energy at other frequencies.

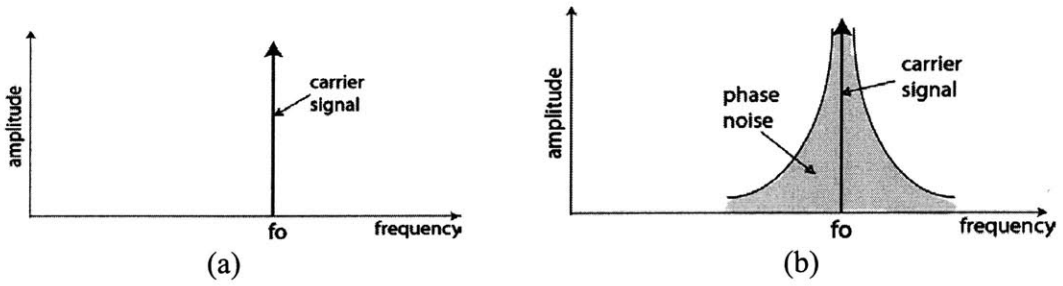

Figure 3-1: Output spectra of: (a) Ideal oscillator; (b) Practical oscillator

Phase noise is usually expressed as the ratio of power at a particular offset frequency from the carrier or center frequency to power at the center frequency. This is the power measured in a 1Hz bandwidth at the frequency offset in consideration. The units of phase noise are dBc/Hz which is read as "decibels below the carrier per hertz."

Phase noise is an important issue in RF systems because it degrades system performance by reducing the signal integrity of their outputs. This effect is seen in both the receiver and transmitter circuitry of wireless communication systems. In the receive path, when the incoming signal is demodulated by convolving it with a local oscillator (LO) signal which has phase noise, an output spectrum similar to that shown in Figure 3-1b is produced [11]. But if an interfering signal close to the desired signal is also present at the input of the receiver circuit, it too will be convolved with the LO signal and will have a profile similar to that in Figure 3-1b. Since both the desired signal and interferer are close in frequency, the "skirts" from the interferer are bound to fall within the

same frequency range as the desired signal. This degrades the signal integrity of the RF system.

Furthermore, a similar situation exists for the transmit path. Suppose an RF system transmits at a particular frequency and the output signal has frequency spectrum similar to that in Figure 3-1b because of phase noise. A receiver operating at a frequency whose magnitude is close to that of the transmitter will be adversely affected because the noise of the transmitted signal will fall within the pass band of the receiver's filter. This reduces the signal integrity and data reliability of the received signal. The situations described above are shown in Figures 3-2 and 3-3.

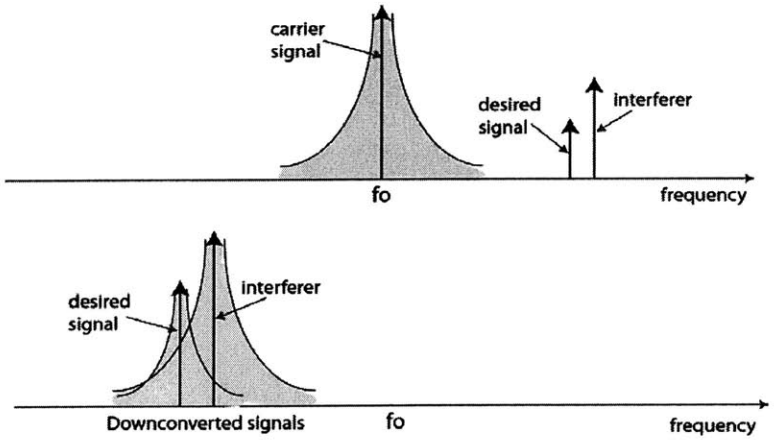

Figure 3-2: Effect of phase noise on the down conversion or demodulation of a signal with a nearby interferer [11].

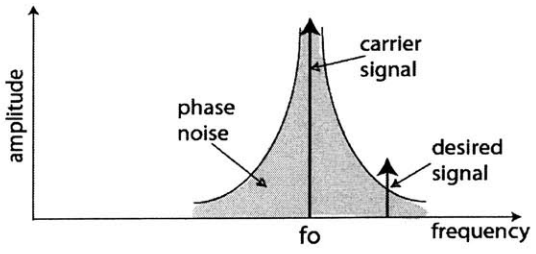

Figure 3-3: Effect of the phase noise of a transmitted signal on the reception of a signal at a nearby frequency [11].

3.2 Phase Noise Models

A number of models have been developed which help the circuit designer to estimate the phase noise introduced into any RF system by the oscillator. These models provide good insight and intuition concerning the various dependencies and trade offs that can be used to reduce phase noise. The use of models which simplify the calculation of phase noise is essential because of the non-linearity and complexity of the processes which generate phase noise in oscillators. Exact expressions which can accurately determine the phase noise are simply impractical for the hand calculations used in circuit design.

3.2.1 The Leeson Phase Noise Model

One such model is a linear time invariant model proposed by D.B. Leeson [2]. This is a relatively simple equation that can be used to calculate the phase noise at a given offset frequency, Δω, from the center frequency:

$$L\{\Delta\omega\} = 10\log\left[\frac{2FkT}{P_{sig}}\left\{1+\left(\frac{\omega_0}{2Q\Delta\omega}\right)^2\right\}\left(1+\frac{\Delta\omega_{1/f^3}}{|\Delta\omega|}\right)\right] \qquad (3\text{-}1)$$

In equation (3-1), F is an empirical fitting parameter whose value varies with oscillator topology and has to be measured; $\Delta\omega_{1/f^3}$ is the boundary between the $1/(\Delta\omega)^2$ and $1/|\Delta\omega|^3$ regions; and P_{sig} is the power of the output signal. This model shows some key characteristics of the phase noise of an oscillator. To reduce the phase noise, signal power or amplitude and Q should be increased, while the noise factor, F, should be reduced. It is for this reason that a lot of effort has been put by RF designers to increase the loaded Q of

the resonator in LC oscillators. Since in general, integrated capacitors of relatively high Q-factors (> 40) are easily available, the above effort leads to maximizing the Q of the integrated inductor since it is usually very low (≈5-10). This arises from the fact that the loaded Q of a tank is mainly determined by the Q of its poorest component, which is usually the integrated inductor.

Leeson's model has the advantage of simplicity and the provision of good design intuition. The RF designer is able to quickly see the trade offs available in the optimization of the performance of his / her oscillator designs. A drawback of this model is the fact that the empirical fitting factor, F, cannot be obtained analytically but must be measured for the given topology. In addition, $\Delta\omega_{1/f^3}$, is not equal to the $1/f$ corner of the active devices or transistors as assumed by this model. Thus, this parameter becomes yet another fitting factor that was historically obtained from measurement [1].

3.2.2 The Hajimiri Linear Time-Variant Phase Noise Model

Some of the problems with Leeson's model are solved by the Linear Time Varying (LTV) model formulated by A. Hajimiri and T.H. Lee [1]. An important property of oscillators which is not accounted for in the Leeson model is the time variance and cyclostationary nature of noise. The response of an oscillator to device noise depends on which point in the period of oscillation this noise is applied. Rather than being time invariant, this observation indicates that LC oscillators are time-varying systems. This fact is illustrated in Figure 3-4 for an ideal oscillator [1].

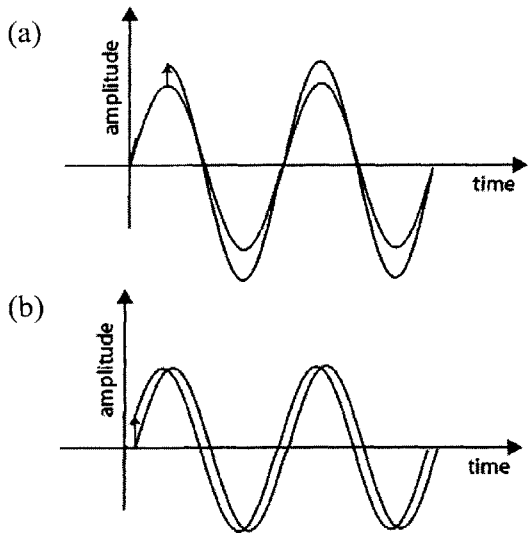

Figure 3-4: Effects of linear time varying properties of oscillators on the impulse response

The figure shows the different responses of an ideal oscillator to an impulse applied at a point near, (a) a voltage maximum and, (b) a zero crossing of the output signal. In 3-4a, it is noticed that when the impulse is applied, there is an abrupt increase in the amplitude with little or no change in the phase of the sinusoidal waveform. Given the fact that all oscillators have some amplitude limiting mechanism, this change in the output voltage magnitude is removed and there is no phase noise. On the other hand, in Figure 3-4b, there is maximum change in the phase but little or no change in the amplitude of the output signal. Thus, it can be concluded that the oscillator is most sensitive to noise at the zero crossing or alternatively, when the amplitude of the output signal is at its mean value. In general, noise impulses occur throughout the period of oscillation and thus, there is always a combination of amplitude and phase perturbations. The response or susceptibility of the oscillator is defined by what is called an impulse sensitivity function, Γ. This function is obtained from simulations in Hspice or SpectreRF by applying a series of small impulses at regular intervals within a period of oscillation and measuring

the change in phase produced. The result is used to calculate the phase noise of the LC oscillator using the equation below [4]:

$$L(\Delta\omega) = 10\log\left(\frac{\Gamma_{rms}^2}{q_{\max}^2} * \frac{\bar{i}_n^2/\Delta f}{2*\Delta\omega^2}\right) \tag{3-2}$$

where Γ_{rms} = rms value of impulse sensitivity function

$q_{\max}$ = maximum charge swing

$\bar{i}_n^2/\Delta f$ = noise current power spectral density

$\Delta\omega$ = offset frequency from carrier

Note that there are no empirical factors which can only be obtained by measurement. Every term in Equation 3-2 can be obtained by hand calculations and simulation. This is an obvious advantage over Leeson's formula. But, the LTV model is not without its drawbacks. It requires a lot of simulation time which increases with the number of components and noise sources. In addition, it does not provide much intuition for hand calculations. In other words, the dependencies which can be used to optimize the design of the resonant tank are not obvious. For instance, the Q-factor of the tank does not appear explicitly in the phase noise expression. Rather, it is embedded in the other terms.

3.2.3 The Rael-Abidi Phase Noise Model

The third phase noise model to be discussed in this section is the J.J. Rael and A.A. Abidi phase noise model [3]. This is a model based on Leeson's linear time-invariant phase noise model. Closed form expressions for the empirical fitting factor, F, in the Leeson phase noise model have been derived for the differential LC oscillator topology shown in Figure 2-2b. Thus, the drawback of obtaining the value of F from meas-

measurements has been removed and the simplicity of Leeson's model can be fully taken advantage of.

Rael's model classifies the device noise which is converted to phase noise into three major categories:

(a) Thermally induced phase noise due to the resonant tank: This is the white noise generated by the parasitic resistances associated with the inductors and capacitors in the resonator. The expression for this component of phase noise is:

$$\mathrm{L}(\Delta f_0) = N_1 N_2 \frac{kTR}{V_0^2}\left(\frac{f_0}{2Q\Delta f_0}\right)^2$$

where $N_1 = 2$; $N_2 = 4$

Δf_0 = offset frequency;

f_0 = center frequency

Q = quality factor of resonant tank;

R = equivalent parallel resistance of resonant tank

V_0 = output signal swing

(b) Thermally induced phase noise due to the differential transistor pair: The channel of the differential pair transistors acts as a resistance. Thus, the drain current serves as a source of noise. The expression for this component of phase noise is

$$\mathrm{L}(\Delta f_0) = \frac{32\gamma I_{BIAS} R}{\pi V_0}\frac{kTR}{V_0^2}\left(\frac{f_0}{2Q\Delta f_0}\right)^2$$

I_{BIAS} = Tail or bias current

(c) Thermally induced phase noise due to the tail current source: This component of phase noise is due to the drain current of the tail bias current source transistor. Once again, this noise is as a result of the fact that the channel of the tail transistor acts like a resistor. The expression for this component of the phase noise is given by:

$$L(\Delta f_0) = \frac{32}{9}\gamma g_{m,TAIL} R \frac{kTR}{V_0^2}\left(\frac{f_0}{2Q\Delta f_0}\right)^2$$

where γ = *noise factor*

$g_{m,TAIL}$ = transconductance of tail current transistor

The problem with this model is that it does not apply to a generic LC oscillator. It was constructed for the specific LC oscillator topology in Figure 2-2b. In addition, no closed form expression for the phase noise produced by flicker noise in the MOS transistors is included in [3]. Despite this fact, the Rael-Abidi model was chosen for this project because of its simplicity and good design intuition. Also, the phase noise of the oscillator will be calculated at an offset of 20MHz which is within the $1/f^2$ region in which flicker noise is insignificant. Thus, significant errors will not be introduced into the analyses of chapter 4. It should be noted that the use of this model restricted the oscillator topology which could be used for the analysis in the later chapters. This does not matter because the goal of this project is to show that a simpler transformer-based architecture can be used to increase the Q-factor of the resonant tank for any oscillator. The oscillator topology in figure 2-2b happens to be the one chosen for analysis. But as will be seen in the next chapter, the analysis and conclusions reached are generic enough to be applicable to any LC oscillator topology.

3.3 Summary

This chapter has provided a basic understanding of the concept of phase noise in LC oscillators. The detrimental effects of phase noise on the performance of wireless communication systems were discussed. Because the conversion of device noise to phase noise is a complicated process, a number of simple models which are used to model phase

noise were presented. These phase noise models were the Leeson linear time invariant model, the Hajimiri linear time varying model and the Rael-Abidi model. The simplicity of the Rael-Abidi model made it the phase noise model of choice for the analysis of the transformer-coupled oscillator in this thesis project. The next chapter will consider a number of techniques which are used to reduce the phase noise in LC oscillators. One of these techniques will be selected for use in the design of an LC oscillator with a center frequency of 5GHz.

Chapter 4

Methods of reducing Phase Noise in LC Oscillators

The problems described in the previous sections make it clear that the reduction of the phase noise introduced into RF systems by oscillators is essential for the design of reliable systems. Some of the methods of reducing phase noise which are currently available are described in the sections below:

4.1 Increase the amplitude and power of the output signal

Increasing the amplitude of the output signal reduces the phase noise of the oscillator because the signal to noise ratio is increased. This arises because the magnitude of the noise remains the same while the output signal amplitude is increased. Alternatively, some methods available in literature seek to obtain the desired signal amplitude with a smaller bias current. A good example of this is the complementary differential LC oscillator in [6]. The use of cross-coupled PMOS transistors in addition to NMOS transistors makes it possible to obtain a larger signal swing for a given bias current than an oscillator using only one set of cross coupled transistors.

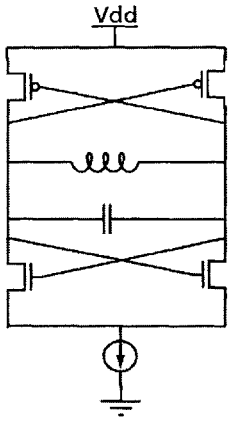

Figure 4-1: Complementary differential LC oscillator

4.2 Reduce the percentage of device noise converted to phase noise

Another method of reducing phase noise is to minimize the effect of the fundamental device noise processes that cause it. An example of this technique is the use of a noise filter to filter out noise at a particular frequency from the output of the oscillator [8]. The noise filter is a simple narrowband circuit which consists of a large capacitor in parallel with the tail current source and an inductor connected between the drain of the tail current transistor and the sources of the differential pair FETs.

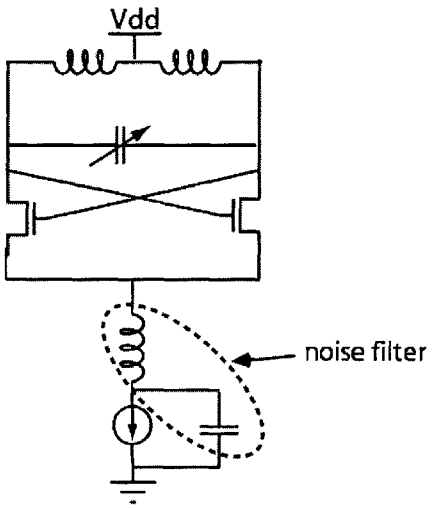

Figure 4-1a: Differential VCO showing noise filter [8]

The capacitor shorts noise frequencies around $2\omega_0$ to ground (ω_0 = center frequency) and prevents this component from producing phase noise. An inductor is introduced into the design to provide a high impedance between the sources of the differential pair FETs and drain of the tail current FET. This prevents the differential pair FETs from loading the resonator when they are in the triode region of operation. Any loading of the resonator will significantly degrade its quality factor, Q, and increase the phase noise of the oscillator. The inductor size is chosen to resonate at a frequency of $2\omega_0$ with the capacitances at the sources of the differential pair FETs. Hegazi asserts in [8] that only thermal noise in the tail current source around the second harmonic of the center frequency produces phase noise. This is the reason for the effort of designing the noise filter to eliminate device thermal noise at this frequency.

4.3 Increase the Q of the resonant tank

As mentioned previously, Leeson's formula shows that the phase noise of an oscillator is inversely proportional to the Q of its resonant tank. Hence, many techniques have been developed to improve the Q of the resonator within the constraints imposed by available technology. In general, this process simplifies to maximizing the Q of the integrated inductor because the Q of these passive components are very low ($\approx$5-10).

One method of increasing the Q of the resonator involves driving it differentially rather than single ended [7]. Consider the equivalent pi model of an integrated inductor in Figure 4-2

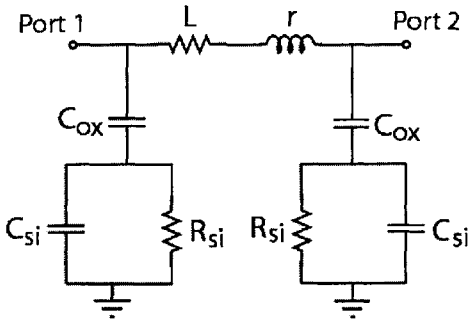

Figure 4-2: Lumped model of integrated inductor [7]

When port 2 is grounded and port 1 is driven by a single ended signal, the shunt RC component on the right is functionally removed from the circuit and the resultant circuit is shown in Figure 4-3a. If both ports of the inductor in Figure 4-2 are driven by two differential signals, the two shunt RC branches are effectively in series because they are connected through the ground terminal. Thus, the inductor model simplifies to the circuit in Figure 4-3b.

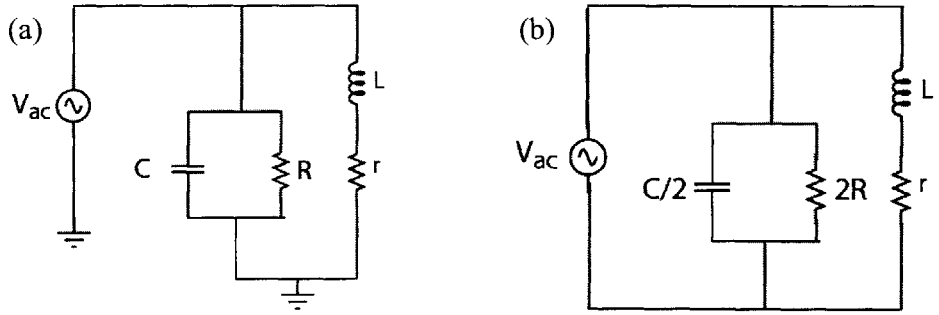

Figure 4-3: (a) Single ended Excitation; (b) Differential Excitation

In the simplified models of the integrated inductor shown in Figure 4-3, the shunt R-C elements model the behavior of C_{OX}, C_{SI} and R_{SI} in the original lumped circuit model of Figure 4-2. The impedance of the shunt R-C element in the single-ended case is $(R+1/\omega C)^{-1}$ while that for the differential case is $(2R+2/\omega C)^{-1}$. At low frequencies, the impedances in both cases are approximately equal. But at higher frequencies, the magni-

tude of the imaginary component of the impedance has a higher value for the differential excitation when compared to the single ended case. This increases the real part and reduces the imaginary part of the tank's input impedance. As a result, the Q of the inductor increases [7].

Another method of increasing the Q of the inductor involves replacing the inductor of the resonator with an integrated transformer. An oscillator topology by Straayer [5] showing this technique can be seen in Figure 4-4.

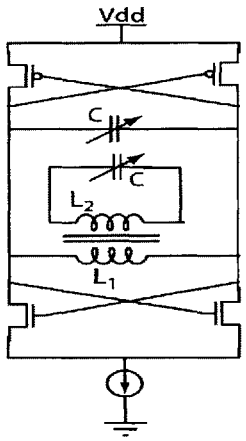

Figure 4-4: Transformer-based CMOS VCO [5]

The oscillator has two resonant LC tanks, one on each side of the transformer with equal capacitance, C. If the coupling coefficient of the transformer, k = 1, the effective inductance of the transformer windings becomes $L + M = 2L$ where $L_1 = L_2 = L$ and mutual inductance, $M = kL$. Straayer asserts that the resultant Q of the transformer windings is double that of a simple inductor with inductance = 2L. The increase in Q can be attributed to the increase in inductance of the transformer windings because of the mutual magnetic coupling between them.

This method of phase noise reduction was selected as the focus of this thesis project because of the potential doubling of the resonator Q-factor and the resultant 6dB re-

duction in phase noise. Furthermore, unlike many of the other techniques discussed in this chapter, the transformer-based approach can be done without the use of additional components. The application of this technique to the design of an LC oscillator will be discussed in more detail in the next chapter.

4.4 Summary

This chapter discusses a number of methods used in practice to reduce the phase noise of an LC oscillator. The techniques were loosely classified into three groups depending on if it focused on; (i) increasing the amplitude of oscillation, (ii) reducing the percentage of device noise which is converted to phase noise, and (iii) increasing the Q of the resonant tank. These classifications were based on the dependencies which can be seen in Leeson's phase noise expression. The third method of phase noise reduction was chosen for the design of the LC oscillator which will be completed in the next chapter.

Chapter 5
Comparison of inductor-based to transformer-based oscillators

There has been considerable interest in the use of transformer-coupled techniques to build low-Q LC resonators. A good example of this technique is presented by Straayer et al in [5]. But this chapter will show that Q-factor enhancement by means of a transformer-coupled resonator can be achieved using a simpler architecture than that presented in [5]. A complementary CMOS VCO constructed using the transformer-coupled resonator discussed in case 3 below will require just a single varactor as compared to two varactors used in [5]. The use of only one varactor eliminates the potential problems which could be introduced by mismatch in the magnitude and tuning range of the varactors. Since no two components can be identical in integrated circuits, it is desirable to use as few devices as possible when designing any system.

Intuitive and analytical explanations for the increase in Q-factor of the resonator when a transformer is used instead of a simple inductor will be presented. A comparison will be made between the phase noise produced by a simple inductor-based oscillator to that produced by a transformer-based oscillator with identical bias currents and active circuit device sizes. It will be shown that the increase in resonator Q obtained by the use of a transformer will lead to a reduction in the phase noise produced by the LC oscillator.

5.1 Case 1: Inductor-based LC Oscillator

This section is divided into two major sub-sections; the design of the LC oscillator and the calculation of its phase noise using Rael's phase noise expressions.

5.1.1 Oscillator Design

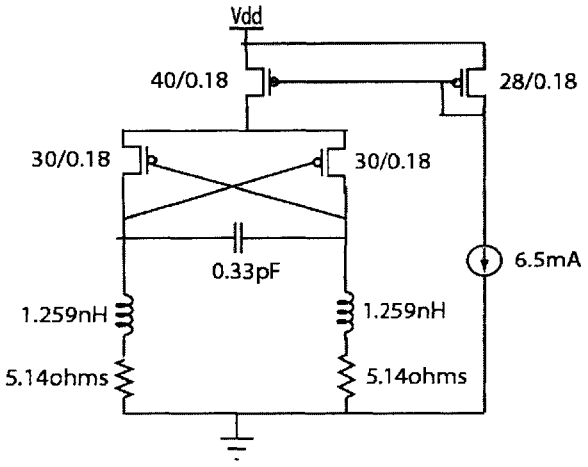

Figure 5-1: Schematic of inductor-based LC Oscillator

The figure above shows the inductor-based oscillator which consists of a resonant tank connected to a negative resistance generator formed by a cross-coupled differential pair of PMOS transistors. The differential pair replenishes the energy lost in the tank resistance as energy is exchanged between the electrostatic field in the capacitor and the magnetic flux in the inductor. Another way of looking at this is to say that the negative resistance provided by the differential pair PMOS transistors cancels out the positive resistance in the tank thereby making the resonator effectively ideal and lossless (ignoring the noise generated by these resistances). The inductor in the resonator was modeled as an ideal inductor in series with a resistance. This simplified model was chosen to make the calculations which will be carried out in this chapter easier to do. To ensure that unrealistic values were not used in the analysis, the inductance and resistance values used in

the resonator were extracted from an actual inductor modeled in ASITIC [9]. For example, if values are chosen such that the Q-factor of an integrated inductor is 50, this will be impractical because standard silicon VLSI processes do not have integrated inductors with such high Q-factors. The oscillator was designed for a center frequency of 5GHz with inductance, L=1.259nH. The series resistance of this inductor was 5.14Ω making the Q = 7.69 at 5GHz. The oscillator was designed as follows:

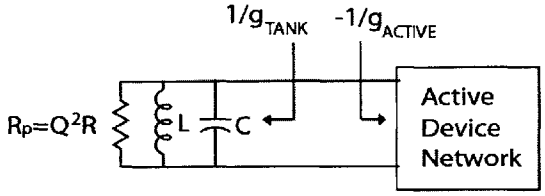

Figure 5-2: Equivalent circuit of LC oscillator

$$L = 1.259nH;\ R = 5.142\Omega\ (extracted\ from\ ASITIC);\ f_0 = 5GHz;\ C = 0.402pF$$

$$Q = \frac{\omega_0 L}{R} = \frac{2\pi f_0 L}{R} = 7.69$$

$$R_P = RQ^2 = 304.08\Omega$$

$$R_{active} = \frac{-2}{g_{m,PMOS}}$$

$$R_{active} \geq -2R_{tank}$$

$$\Rightarrow g_{m,PMOS} \geq \frac{1}{R_{tank}}$$

$$\text{Set } g_{m,PMOS} = \frac{2}{R_{tank}} = \frac{2}{304.8} = 6.577mS$$

$$V_{SWING} = I_{BIAS} * R_P \Rightarrow I_{BIAS} = \frac{V_{SWING}}{R_P} = \frac{2}{304.08} = 6.57mA$$

In the calculations above, the Q of the resonator was taken to be $\frac{\omega_0 L}{R}$. This is strictly the Q of the inductor. But in practical oscillators, the Q of the inductor is much smaller (<10) than the Q of the capacitor (>40). Since the Q of a resonant tank is usually

limited by the component with the smallest Q, it is a good approximation to assume the Q of the tank is equal to the Q of the inductor. A more rigorous analytical proof of why this statement is true can be seen in [12].

It is safe to assume that the transistors in the active device network are velocity saturated during much of the oscillation period because of the supply voltage (1.8V) and channel length (0.18μm). With this combination of supply voltage and device size, the electrostatic field in the transistors is about 10V/μm. This electrostatic field is large enough to push these transistors into the velocity saturation regime. Thus, the square law I-V relationship for the MOSFET is no longer valid and cannot be used to calculate the transistor width required to obtain the required transconductance of gm,PMOS = 6.577mS when the tail current, IBIAS = 6.57mA. The required W/L ratio for the differential PMOS transistors is obtained from a SpectreRF simulation of the circuit shown in Figure 5-2b.

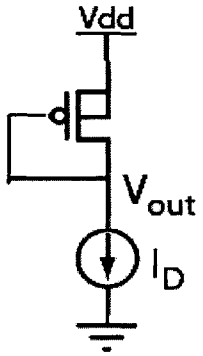

Figure 5-2b: Diode connected PMOSFET used to obtain the required W/L ratio.

This circuit consists of a diode connected PMOSFET with a DC current source connected to its source terminal. The magnitude of the current source is set to 6.57mA which is the required bias current. Next, the width of the PMOSFET is swept through a range of values and the amplitude of the output voltage, v_{out} is recorded.

The resistance of the diode-connected PMOSFET $= \frac{1}{g_m} \| r_o = \frac{1}{g_m}$ (assuming $\frac{1}{g_m} << r_o$).

The transconductance can be obtained from $g_m = \frac{i_d}{v_{out}}$. The required width to obtain $g_m = 6.57mS$ is read from a graph of g_m versus width and was found to be about 30μm. This is the PMOS transistor width needed for startup of the oscillator.

5.1.2 Calculation of Phase Noise

The phase noise was calculated using expressions by Real et al [3] which calculate the phase noise due to thermal device noise. The use of these expressions is justified because the phase noise will be calculated at an offset of 20MHz. At this offset, the transistors are in the $1/f^2$ region where phase noise is dominated by thermal noise and falls off at -20 dB/decade. Flicker noise is more significant at frequency offsets close to the center frequency.

The calculations below describe the computation of phase noise for the oscillator topology in Figure 5-1. It is divided into 3 major noise contributors: thermal noise in the parasitic resistance of the resonator, thermal noise in the tail current transistor, and thermal noise in the differential pair PMOS transistors.

Resonator Noise

$$L(\Delta f_0 = 20MHz) = N_1 N_2 \frac{kTR}{V_0^2}\left(\frac{f_0}{2Q\Delta f_0}\right)^2 = 6.653*10^{-16}$$

where $N_1 = 2; N_2 = 4$

$$V_0 = V_{SWING} = 2V$$

Tail Current Noise

$$L(\Delta f_0 = 20MHz) = \frac{32}{9}\gamma g_{m,TAIL} R \frac{kTR}{V_0^2}\left(\frac{f_0}{2Q\Delta f_0}\right)^2 = 1.484*10^{-15}$$

where γ = *noise factor* $= 2.5; g_{m,TAIL} = g_{PMOS} = 6.577mS$

Differential Pair Noise

$$L(\Delta f_0 = 20MHz) = \frac{32\gamma I_{BIAS} R}{\pi V_0}\frac{kTR}{V_0^2}\left(\frac{f_0}{2Q\Delta f_0}\right)^2 = 2.093*10^{-15}$$

$$L_{TOTAL}(\Delta f_0 = 20MHz) = 6.653*10^{-16} + 1.484*10^{-15} + 2.093*10^{-15}$$
$$= 4.24*10^{-15}$$
$$\text{Phase noise} = 10\log(L_{TOTAL}(\Delta f_0 = 20MHz)) = -143.7\, dBc/Hz$$

The oscillator in Figure 5-1 was also simulated using Cadence's SpectreRF simulator. The phase noise obtained was -147.4 dBc/Hz at 20MHz offset from a center frequency of 5GHz

5.2 Case 2: LC Oscillator with Transformer-Based Resonator which includes a passive secondary LC tank

This topology is similar to that presented by Straayer et al in [5]. The inductive elements in the resonator are replaced by a transformer. The distinctive characteristic of this archi-

tecture is the presence of an additional resonant LC tank which is "floating" or electrically isolated from the rest of the circuit. The oscillator in Figure 5-3 is a PMOS only version of the fully complementary differential oscillator in [5]. Straayer asserts that if the coupling coefficient of the transformer, k = 1, the Q of the transformer windings will double in magnitude. This will lead to a reduction in the phase noise of the oscillator because of the inverse square relationship between phase noise and tank Q. More details about this oscillator topology are presented in Appendix A.

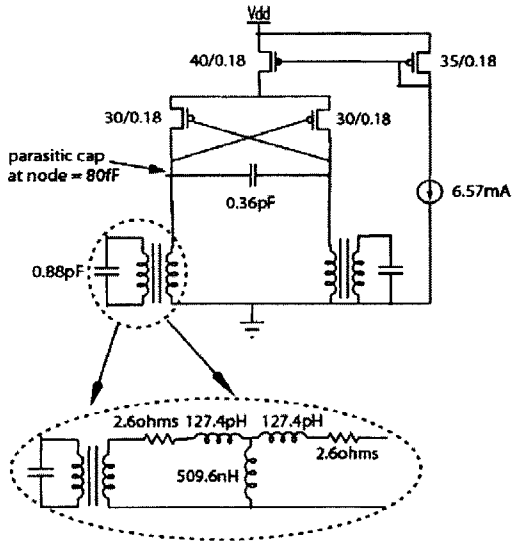

Figure 5-3: Transformer-based LC VCO with passive secondary LC tank.

The circuit shown above was simulated in SpectreRF to get an estimate of the phase noise produced by this oscillator. The simulation results showed a phase noise of -152.2 dBc/decade at a 20MHz offset from the center frequency of 5GHz.

5.3 Case 3: LC Oscillator with Simple Transformer-Based Resonator

This section presents an alternative topology to case 2 which also employs a transformer-coupled resonator. Figure 5-4 shows that the inductor-based oscillator topology in case 1 was modified by replacing the inductors in the resonator with a transformer. The transformer windings will serve as the inductive elements in the resonant tank. The phase noise of this modified oscillator topology will be recalculated to see if any reduction in phase noise is obtained. In addition, a comparison will be made between the phase noise generated by the transformer-based oscillator topologies of case 2 and case 3.

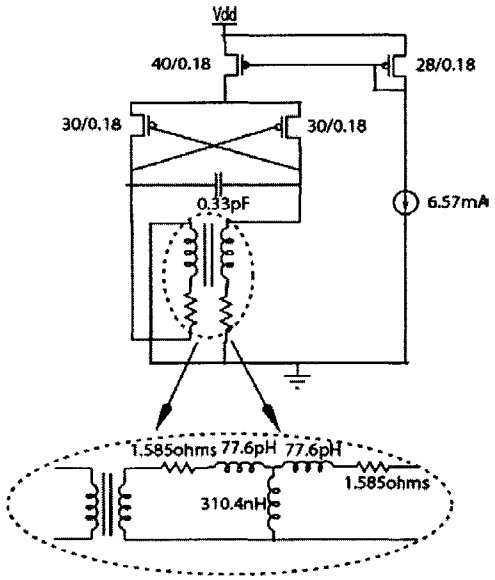

Figure 5-4: LC oscillator with transformer-based resonator

5.3.1 Explanation for Increase in Q with Transformer-Based Resonator

When two current carrying conductors are in close proximity to each other, and their respective currents flow in such a direction that makes their respective magnetic

fields reinforce each other, then it is true to state that their self inductances will decrease while their mutual inductances will increase. However, the increase in mutual inductance is usually more than the decrease in self inductance. Therefore, it is valid to conclude that the effective or net inductance of the two current carrying conductors in close proximity to each other will increase. Intuitively, if this net increase in inductance is not accompanied by a corresponding increase in the series resistance of the inductor, an increase in the effective Q-factor of the inductor is expected. This assertion is proved using the analysis that follows:

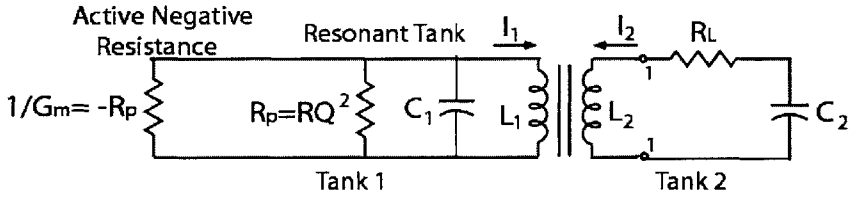

Figure 5-5: Equivalent circuit of transformer-based resonator

At resonance, the negative reactance of the capacitor and positive reactance of the inductor in Tank 1 of Figure 5-5 will cancel out thus making the tank to have a purely real impedance. Furthermore, the mode of operation of the oscillator ensures that the negative resistance provided by the active device network is approximately equal to the real impedance of the tank. Thus, looking into the terminals 1-1 of Tank 2, the negative resistance of the active device network connected to Tank 1 cancels out its positive impedance. Therefore, from a large signal point of view, no impedance is reflected from Tank 1 to Tank 2. This ensures that the series resistance of the inductor in Tank 2 remains unchanged. But the magnetic coupling between the inductors in the two tanks will cause a voltage, V_1 to be induced in Tank 2 due to the magnetic flux produced by current

flowing in Tank 1. This voltage appears as a mutual inductance which is in series with the self inductance of the inductor in Tank 2. Thus, writing KVL for the mesh in Tank 2,

$$\left(sL_2 + R_L + \frac{1}{sC_2}\right)I_2 + V_1 = 0$$

$$\left(sL_2 + R_L + \frac{1}{sC_2}\right)I_2 + skL_1I_1 = 0$$

$$sL_1I_1 + skL_2I_2 + \left(R_L + \frac{1}{sC_2}\right)I_1 = 0$$

$$sL(1+k)I + R_LI + \frac{1}{sC_2}I = 0$$

$$where\ I_1 = I_2 = I\ and\ \ L_1 = L_2 = L$$

Thus, the effective inductance of the inductive element in Tank 2 has increased to a value $(1+k)L_2$. The final equivalent circuit is shown in Figure 5-6. It should be noted that the series resistance, R_L has remained the same while the effective inductance has increased. The new effective value of the Q-factor is calculated as:

$$L_{case2} = (1+k)L_2 = (1+k)L_{case1}$$

$$\Rightarrow Q_{case2} = \frac{\omega_0 L_{case2}}{R_{L,case2}} = \frac{\omega_0(1+k)L_{case1}}{R_{L,case2}} = (1+k)Q_{case1}$$

$$= (1+0.8)*7.69 = 13.85$$

An increase in Q by a factor of (1+k) = 1.8 is obtained by using a transformer instead of a simple inductor. This is the same factor by which the inductance of the transformer windings is increased. It was pointed out previously that Leeson's phase noise formula [2] indicates that the phase noise generated by an oscillator is inversely proportional to the square of the resonator Q-factor. Consequently, a reduction in phase noise is expected as the calculation in the next section will show.

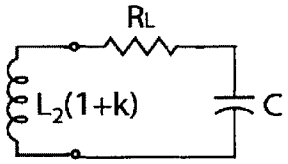

Figure 5-6: Final equivalent circuit of transformer-based resonator

It should also be noted that the windings of the transformer shown in Figure 5-5 above are driven with a polarity that ensures that the magnetic flux produced by one winding reinforces the flux of the other so that the effective inductance is increased by a factor of $(1+k)$.

5.3.2 Oscillator Design

In order to facilitate easy comparison between the current topology and that in case 1, it is necessary for both oscillators to operate with identical specifications. The transformer-based topology was designed so that the amplitude of the output signal, the bias current, and the center frequency are identical to that of the oscillator in case 1. To ensure that both topologies have the same output signal amplitude for the same bias current, their respective resonators must have the same equivalent parallel resistance at resonance. This stems from the fact that the amplitude of the output signal of an oscillator is proportional to the product of the bias current and equivalent parallel resistance [4]. For Tank 1 in Figure 5-5,

$$V_{swing} = I_{BIAS} * R_P$$
$$where\ I_{BIAS} = tail\ bias\ current$$
$$and\ R_P = \text{equivalent parallel resistance}$$

The design methodology was first to set the desired value of $R_P = 304\Omega$ needed to get a particular output swing for a given bias current. Then, the series resistance of the

inductor is calculated using the new effective Q-factor. Next, the value of the inductor which will have this series resistance is calculated and a suitable capacitance value is chosen to set the resonant frequency of the tank equal to 5GHz. This series of design steps is shown below:

$$If\ V_{swing} = 2V\ and\ I_{BIAS} = 6.57mA\ (\text{same as case 1})$$

$$Then,\ R_{eff} = \frac{V_{swing}}{I_{BIAS}} = 304\Omega$$

$$Also,\ R_p = R_{eff} = R_{L,case3}Q^2_{case3} = R_{L,case3} * 13.85^2 \Rightarrow R_{L,case3} = 1.585\Omega$$

Since for a practical inductor R scales linearly with L,

$$L_{case3} = L_{case1}\frac{R_{L,case3}}{R_{L,case1}} = 1.259nH * \frac{1.585}{5.142} = 0.388nH$$

$$L_{eff} = (1+k)L_{case3} = 698.5pH$$

$$from\ f_0 = \frac{1}{2\pi\sqrt{LC}} = 5GHz, C = 1.45pF$$

The calculation above concludes the design of the resonant tank in case 3. The active device network which consists of the differential PMOSFET pair and the tail bias current FET is the same as that used in case 1.

5.3.3 Phase Noise Calculation

Rael's closed form phase noise expressions [3] were used in calculating the phase noise even though the oscillator topology under consideration is different from that for which the expressions were derived. This was justified because the topology of case 3 is similar to that in case 1 if the two windings of the transformer are taken as the two inductive elements in resonant tank. The calculation of phase noise is shown below:

Resonator Noise

$$L(\Delta f_0 = 20MHz) = N_1 N_2 \frac{kTR}{V_0^2}\left(\frac{f_0}{2Q\Delta f_0}\right)^2 = 2.05*10^{-16}$$

where $N_1 = 2; N_2 = 4$

$V_0 = V_{SWING} = 2V$

Tail Current Noise

$$L(\Delta f_0 = 20MHz) = \frac{32}{9}\gamma g_{m,TAIL} R \frac{kTR}{V_0^2}\left(\frac{f_0}{2Q\Delta f_0}\right)^2 = 4.55*10^{-16}$$

where $\gamma = noise\ factor = 2.5; g_{m,TAIL} = g_{PMOS} = 6.58mS$

Differential Pair Noise

$$L(\Delta f_0 = 20MHz) = \frac{32\gamma I_{BIAS} R}{\pi V_0}\frac{kTR}{V_0^2}\left(\frac{f_0}{2Q\Delta f_0}\right)^2 = 6.52*10^{-16}$$

$$L_{TOTAL}(\Delta f_0 = 20MHz) = 2.05*10^{-16} + 4.55*10^{-16} + 6.52*10^{-15}$$
$$= 1.31*10^{-15}$$

$$\text{Phase noise} = 10\log(L_{TOTAL}(\Delta f_0 = 20MHz)) = -148.83\,dBc/Hz$$

The circuit in Figure 5-4 was simulated using Cadence's SpectreRF tool and the phase noise obtained was -152.58dBc/Hz @ 20MHz offset. The difference of 3.7dB between the calculated and simulated values can be attributed to the approximations used for the hand calculations. This discrepancy is not important because this chapter is focused on determining the difference and improvement obtained by using a transformer-based resonator rather than the absolute value of the phase noise. As long as the errors introduced in the hand calculation are identical in all the LC oscillator topologies considered in this chapter, the difference between the calculated and simulated values of phase noise is not an issue. Note that if the above calculations are repeated for Tank 1 while looking into the terminals of Tank 2, the same results will be obtained.

5.4 Analysis of results

The results from all three resonator topologies are summarized in table 5-1 below:

	Phase Noise (dBc/Hz) at a 20MHz offset from a 5GHz center frequency			Phase Noise Difference (dB)	
	Case 1	Case 2	Case 3	Case 1 – Case 3	Case 2 – Case 3
Calculated	-143.7	-148.9**	-148.8	5.1	**0.1
Simulated	-147.4	-152.2	-152.6	5.2	0.4
Relative Difference (dB)	3.7	3.3**	3.8		

Table 5-1: Summary of results in all three topologies of the LC oscillator.

The above table shows that a 5.1dB reduction in phase noise is obtained by replacing the inductor in the resonator of an LC oscillator by an integrated transformer. This result makes intuitive sense when we consider the dependence of phase noise on the Q of the resonant tank using Leeson's phase noise expression [2].

$$L\{\Delta\omega\} = 10\log\left[\frac{2FkT}{P_{sig}}\left\{1+\left(\frac{\omega_0}{2Q\Delta\omega}\right)^2\right\}\left(1+\frac{\Delta\omega_{1/f^3}}{|\Delta\omega|}\right)\right]$$

$$\Rightarrow L\{\Delta\omega\} \propto 10\log\left(\frac{1}{Q^2}\right)$$

Since the Q of the inductor in the transformer based resonator of case 3 is greater than that of the simple resonator in case 1 by a factor of 1.8, the difference in phase noise between the two cases should be,

$$\Delta L\{\Delta\omega\} = 10\log\left(\frac{1}{1.8^2}\right) = 5.1dB$$

**see Appendix A

This conclusion agrees with the results summarized in Table 5-1 above. It is also worth mentioning that the phase noise of the oscillator can be reduced even further by driving the transformer windings differentially. This will increase the Q-factor of the transformer windings as discussed in Section 4.3.

The results obtained in this chapter have proved that the phase noise of an oscillator can be reduced by using a transformer-based resonator architecture which is simpler than that presented in [5]. This conclusion is drawn from Table 5-1 which shows that the phase noise from SpectreRF simulations of case 2 is -152.2 dBc/Hz and that of case 3 is -152.6 dBc/Hz with both values measured at a 20MHz offset from the center frequency of 5GHz. Case 3 has the advantage of requiring only one capacitor as opposed to two capacitors in case 2. This fact eliminates the problems that could arise from the mismatch in the magnitude of the capacitors. In the case of a VCO, the capacitors will be replaced by a varactor. The use of two varactors could also include problems due to a mismatch in the magnitude and tuning range of the varactors. This is not an issue for the oscillator topology in case 3 because only one varactor is required.

5.5 Summary

In this chapter, it was proved that the simpler transformer-based oscillator referred to as case 3 produces the same phase noise as the alternative topology similar to that proposed by Straayer et al [5] and referred to as case 2 in the text. This is an important conclusion because the oscillator topology in case 3 requires the use of just one capacitor as opposed to the two capacitors required for the topology in case 2. In the case of a VCO where the capacitors are replaced by varactors, the use of two varactors in case 2 could introduce

problems due to a mismatch in the magnitude and tuning ranges of the varactor. This is not an issue in the transformer-based oscillator of case 3 which requires just one varactor.

In addition, it was verified that the phase noise of an LC resonator is reduced by replacing the inductors in the resonator by a transformer. The mutual coupling between the windings of the transformer increases their Q-factors and reduces the phase noise of the oscillator in accordance with the inverse squared relationship between the two quantities seen in Leeson's phase noise formula. The next chapter will discuss the modeling and design of the integrated inductors and transformers which are the most critical components in the design of an LC oscillator.

Chapter 6

Design of Inductor and Transformer

The previous chapters have established the fact that the use of transformers as the inductive elements in LC resonators leads to an increase in Q-factor and a reduction in the phase noise of LC oscillators. Despite this fact, it is important to verify that the transformer structures required to produce this increase in Q-factor can actually be constructed in a standard VLSI process. This is especially important given the size constraints imposed by the requirements of multi-GHz frequencies used in today's RF systems. Thus, it is crucial to carefully design and optimize the transformer to get as high a value of quality factor, Q, as possible. Integrated inductors and transformers tend to have poor Q-factors because they are constructed from the thin metal traces available in standard VLSI processes. Although much better inductors and transformers can be constructed off chip, it is desirable to put these components on chip to reduce costs and improve the miniaturization of RF systems for mobile applications. Moreover, off chip inductors require the use of bond wires for connection to the on chip components of the RF system. At multi-GHz frequencies, bond wires are effectively inductors which are in series with the off chip inductor used for the application in question. Because there is a significant variation in the length of bond wires, a considerable variation in the effective inductance in the system is produced. This state of affairs is undesirable for applications which require a fairly accurate carrier frequency for the reliable transmission of data. Although this

variation can be reduced by the use of the capacitor banks shown in Figure 2-7, resonators using this technique tend to have lower quality factors.

An integrated inductor consists of a spiral of metal which can be made in various geometries or shapes including circle, square, and N-sided polygons. On the other hand, an integrated transformer consists of a spiral of inter-wound conductors or metal traces lying in the same plane or stacked one on top of the other in different planes. These conductors are placed very close to each other to ensure that there is sufficient magnetic coupling between them. Thus, in a typical VLSI process, transformers with coupling coefficients of 0.7 or greater can be made. The mutual inductance of the transformer is proportional to the peripheral length of the conductors, spacing and width of the metal traces, and the substrate thickness [10]. Inductors and transformers are usually made from the top level metal because it has a larger thickness and is furthest away from the substrate. The larger thickness ensures that the inductor or transformer winding will have a lower series resistance and thus, a higher Q-factor. The larger distance from the substrate reduces the effects of parasitic capacitances and resistances on the operation and frequency response of the inductor or transformer.

6.1 Transformer Layouts

Some of transformer layouts or winding configurations which are available in literature are shown in figure 6-1. Each one of these square layouts is defined by a number of parameters which include: n = number of turns; s = spacing between metal traces; w = width of metal trace; d_{out}= outer conductor length; and d_{in} = inner conductor length.

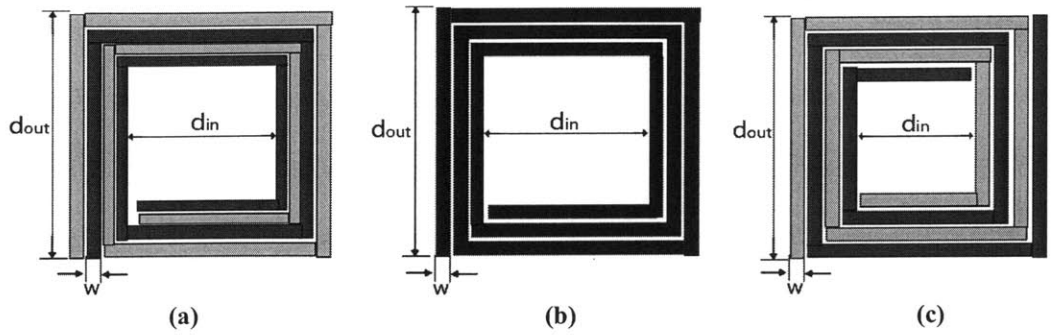

Figure 6-1 [1]: Diagram of various transformer topologies: (a) Parallel (Shibata) configuration; (b) Overlay (Finlay) configuration; (c) Inter wound (Frlan) configuration

The parallel conductor (Shibata) configuration is made up of two conductors which are inter-wound and lie in the same plane. This is done to promote edge coupling between the primary and secondary windings which increases the coupling coefficient, k. If this topology is used as shown in figure 6-1a, the total unwound lengths of the primary and secondary windings will not be equal. This problem can be solved by coupling two such transformers of identical dimensions. The inner spiral of one transformer is connected in series with the outer spiral of the other transformer. Since the Shibata configuration will potentially require more area that the other topologies, it was not used in this project.

Figure 6-1b shows the Overlay (Finlay) winding configuration in which the two windings are on different metal layers and are staked one on top of the other. This has the advantage of high coupling coefficient, k, because magnetic coupling is achieved both from the edges and the flat surfaces of the metal traces. Thus, coupling coefficients close to 0.9 are easy to achieve with this configuration. In addition, a relatively smaller area is required to achieve the same inductance as the other layouts. The disadvantage of this winding configuration lies in the fact that the primary and secondary windings are constructed with different metals which have different sheet resistances. Thus, the Q-factors

of the two windings will be different which is not acceptable for an oscillator topology which requires a symmetric resonator. Therefore, this winding configuration was also not used in the construction of the transformer-based resonator.

Figure 6-1c shows the Inter wound (Frlan) configuration in which the primary and secondary windings are identical and lie in the same plane. This configuration ensures that when both windings have the same number of turns, they are electrically identical. In addition, this configuration has the advantage of placing the terminals of the transformer at opposite ends which makes it easier to connect the transformer to other components in the system. The Frlan winding configuration was selected as the most suitable configuration for the resonant tank of the oscillator.

6.2 Design of Inductor and Transformer

The design and optimization of the integrated inductor and transformer was achieved using an electromagnetic simulator called ASITIC [9]. This EM simulator models the physical and electromagnetic behavior of integrated inductors by utilizing circuit and network analysis techniques to derive a frequency-independent lumped circuit. The tool can rapidly search the parameter space of possible inductors in an optimization problem to select a particular configuration that satisfies the requirements of the current application. The value of inductance to be used in the optimization process was chosen so that the final dimensions of the transformer were realistic and could be constructed in a typical silicon VLSI process.

Initially, ASITIC was used to attempt the design of an inductor with L = 1.259nH and a transformer with primary and secondary winding inductance, L = .388nH. These

are the same values used in the analysis of Chapter 5. To facilitate easy comparison and verification of the analysis of Chapter 5, the transformer was designed so that the Q-factor of its primary and secondary windings was approximately equal to that of the inductor used in the differential LC oscillator of Figure 5-1. The parameters of the inductor and transformer which were designed are shown in Table 6-1 below:

Name of Structure	**Inductance per winding**	**Number of Turns**	**Width**	**Spacing**	**Length**	**Q-factor**
Simple Inductor	3.13	3	7.2	3	200	7.1
Transformer	1.1	3	16	1	200	7.0 k=.66

Table 6-1: Dimensions of Inductor and Transformer used in analysis

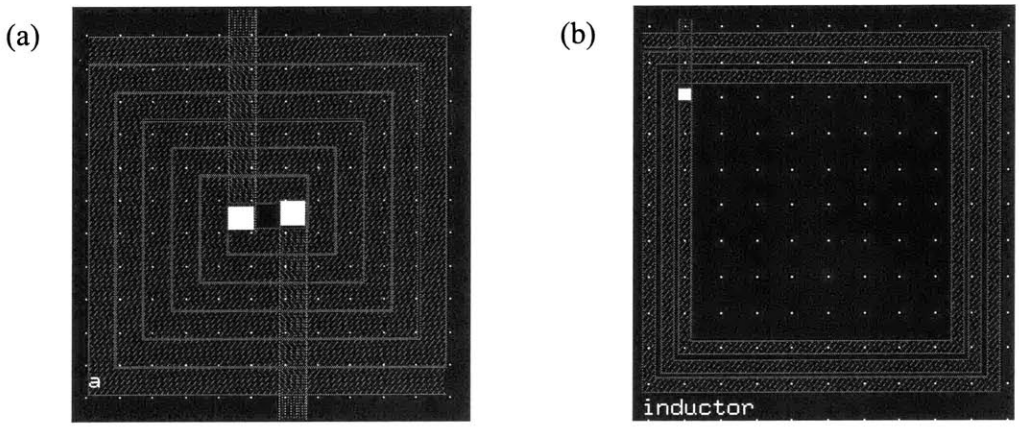

Figure 6-2: ASITIC Layout of (a) inductor; (b) transformer used in design of oscillator.

Note that the inductor and transformer which were used in the final design and shown in Table 6-1 are different from that used in Chapter 5. These changes were made because considerable difficulty was encountered in the design of a transformer with a small inductance, but high coupling coefficient, k, and quality factor, Q. Since the inductance of an inductor (or transformer winding) is proportional to its total unwound

length, a small inductance is obtained if the total unwound length of the transformer winding is small as well. But a large number of turns is required to obtain a good coupling coefficient, k. Therefore, in order to obtain a good coupling coefficient and still have a relatively small self inductance, it is necessary to use a transformer with small outer length, d_{out}, and relatively narrow metal traces. Unfortunately, the use of narrow metal traces leads to a significant reduction in the Q-factor of the transformer due to an increase in series resistance. A large number of simulations in ASITIC showed that it is difficult to design a transformer whose windings have a small inductance, L = .388nH, a Q-factor = 7.69, and a high coupling coefficient, k=0.8.

A different design methodology had to be used because of the problem discussed in the previous paragraph. First, a transformer with an acceptable coupling coefficient and quality factor was selected and modeled in ASITIC. This value was selected arbitrarily with the loose constraint of keeping the transformer winding inductance as low as possible. Next, the inductor was designed to have an inductance greater than that of the transformer by a factor of $(1+k)^2$. The reason this factor was chosen is to ensure that both transformer and inductor have the same equivalent parallel resistance at the same resonant frequency.

$$Q_{transformer} = (1+k)Q_{inductor}$$

$$R_{parr,inductor} = Q_{inductor}^2 R_{inductor}$$

$$R_{parr,transformer} = Q_{transformer}^2 R_{transformer}$$

For easy comparison between the inductor-based and transformer-based resonator, it is necessary to set $R_{parr,inductor} = R_{parr,transformer}$

$$\Rightarrow Q_{inductor}^2 R_{inductor} = Q_{transformer}^2 R_{transformer}$$

$$\therefore R_{inductor} = \frac{Q_{transformer}^2 R_{transformer}}{Q_{inductor}^2} = \frac{(1+k)^2 Q_{inductor}^2 R_{transformer}}{Q_{inductor}^2} = (1+k)^2 R_{transformer}$$

Since the inductance of a practical inductor is approximately proportional to its resistance, it implies that $L_{inductor} = (1+k)^2 L_{transformer}$. The value of transformer winding inductance was chosen with the additional constraint that the size of the inductor in the differential inductor-based LC oscillator is limited by the minimum tank capacitance available in the resonator. This capacitance is the drain junction capacitances of the differential pair MOSFETs. Furthermore, in a voltage controlled oscillator, it is desirable to have as large a tuning range as possible. Thus, it is important to choose the value of the inductance such that a small proportion of the tank capacitance is made up of the drain junction capacitance whose magnitude is constant and cannot be varied like a varactor.

6.3 Constraints of Transformer design for high speed applications

The design of the transformer in this chapter brings up a significant issue for high speed applications which have operating frequencies in the multi-GHz range. At these frequencies, the values of the inductors and capacitors tend to be small. Small inductance values have to be used to ensure that the tank capacitance is large enough to prevent a large percentage of it from being composed of the low Q, drain junction capacitances of the differential pair PMOS transistors. The tuning range of an integrated LC VCO is significantly reduced if a large percentage of its tank capacitance is made up of this drain junction capacitance. In order to keep the Q-factor of the transformer windings large, a transformer with a small number of turns (N < 2) and large width metal traces will have to be used. This statement is true because as the number of turns in a spiral inductor is increased, the series resistance increases significantly faster than the inductance. The in-

ner turns of the inductor add more resistance than inductance and this reduces the ratio of the total inductance to the total resistance. If a spiral with few turns and wide metal traces is used, the transformer will have a smaller coupling coefficient and the increase in Q-factor obtained by using a transformer-coupled resonator will be reduced.

In order to increase the coupling coefficients in transformers used for these high speed applications, it is necessary to use a transformer with a large number of turns ($N > 4$). Obviously, the values of N quoted in this section apply only to the current design and will scale with the required inductance and operating frequency of a particular application. From a geometric standpoint, if the area is fixed or limited, the number of turns can only be increased by using metal traces of smaller width. The drawback is the series resistance of the metal windings increases thus reducing the Q-factor. Therefore, a coupling coefficient, k, and Q-factor tradeoff in the design of these integrated transformers is observed.

6.4 Issues of optimization of area of inductor versus transformer

The previous sections have analyzed the boost in the Q-factor by using an integrated transformer rather than a simple inductor in the resonator. But, the optimization of the area occupied by these passive components has not been looked into. This issue is important because in a modern silicon VLSI process, there it is desirable to use the minimum area possible for the passive components. Inductors and transformers are relatively large structures which take up a significant area of the silicon die. Thus, it is important to design a structure which satisfies the requirements of the application but takes up the

least area possible. The next issue to investigate is to see if an advantage can still be derived by using a transformer if there is a constraint on the area available.

Analyzing the simulation results from ASITIC, it was observed that the individual windings of the transformer tend to have a lower Q-factor than a single inductor with equal area when the number of turns in the transformer is set so that there is a sufficiently high coupling coefficient ($k > 0.7$). In general, the number of turns, N, had to be set to a value greater than or equal to 3 before a coupling coefficient, $k > 0.7$ could be obtained. This can be attributed to the fact that the inner traces of the transformer add more negative mutual inductance while the increased unwound length leads to an increase in the series resistance. As a result, the inductance of the transformer winding does not increase as quickly as its series resistance and thus, there is a reduction in the ratio of the inductance to the resistance. This makes the transformer winding to have a lower Q-factor. On the other hand, a spiral inductor does not have any constraints on the number of turns because there is no requirement to have a high coupling coefficient. This makes it possible to obtain higher Q-factors by reducing the number of turns of the inductor.

If the area of the inductor and width of the metal traces are kept constant, the Q-factor of an inductor is inversely proportional to the spacing between the metal traces. This is shown in the plot in Figure 6-4 below for an inductor with d_{out}=173μm; w=11.8μm; n=2.25:

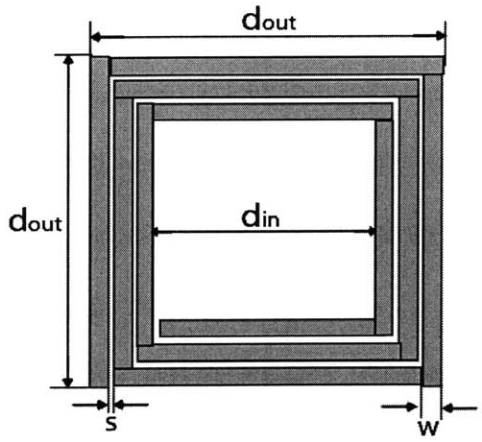

Figure 6-3: Diagram of inductor indicating various parameters.

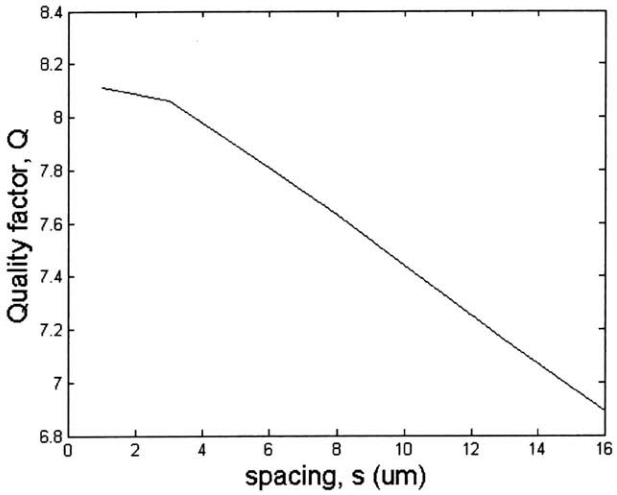

Figure 6-4: Quality factor Q, versus spacing, s for an inductor of fixed area.

Note that when the area or external length, d_{out} is fixed while the spacing s, is increased, the total unwound length of the inductor reduces. This also leads to a reduction in the effective inductance. This fact makes it important to investigate whether the boost in Q-factor due to the magnetic coupling between the transformer windings is large enough to offset the inherent lower Q-factors of these windings. A series of simulations were done with ASITIC in which the area of the inductors and transformers were kept constant while other parameters such as spacing and line width were varied to obtain the largest

Q-factor possible within these constraints. These simulations showed that the best Q-factor obtained for an inductor was larger than the best Q-factor for a transformer by about 1. For a coupling coefficient, $k > 0.6$, a considerable increase in the Q-factor is still obtained by using a transformer-coupling resonator. This result indicates that there is still a significant advantage to using a transformer instead of a simple inductor in the resonator of an LC oscillator.

The overlay transformer layout has the advantage that for a given area, we can fully optimize the Q-factor without hurting the coupling coefficient k, since the magnetic coupling is mainly through the flat surfaces of the two windings. The same cannot be said for the Frlan winding configuration in which we have a direct tradeoff between coupling coefficient, k, and Q-factor as discussed in the last section. Thus, the overlay configuration will be suitable for oscillators with a topology similar to case 3 in the previous chapter or one that does not require a symmetric resonator.

6.5 Summary

This chapter looked into the modeling and design of integrated inductors and transformers. The discussion was motivated by the inherently low Q inductors that are available in standard silicon processes due to the thin dimensions of the metal traces from which they are made. An important tradeoff between the coupling coefficient and quality factor of integrated transformers was revealed. This tradeoff is due to the fact that transformers with high coupling coefficients require a large number of turns while transformers with high quality factors require a smaller number of turns to reduce the series resistance. Even though the series resistance of a transformer with a large number of turns could be

reduced by increasing the width of its metal traces, this measure would increase the parasitic capacitance coupling between the transformer and the silicon substrate. The increase in capacitance will reduce the self resonant frequency and will limit the transformers upper frequency of operation. This state of affairs is undesirable for high speed applications. The next chapter will look into the effects of mismatch in the inductance of the transformer windings on the phase noise of the LC oscillator.

Chapter 7

Effects of mismatch in the passive components of the resonator

7.1 Introduction

In any standard VLSI process, there are tolerances and process variations that cannot be eliminated. For instance, it is impossible to design the windings of a transformer to be geometrically identical. Thus, the effects of mismatch in the inductance of the transformer windings on the change in Q-factor and hence, the phase noise of the LC oscillator should be investigated.

7.2 Calculation of Phase Noise with 20% Mismatch in the inductance of the transformer windings

Consider a 20% mismatch between the expected inductance and the actual inductance value of the transformer windings of the oscillator topology in Figure 5-4 which has been redrawn in Figure 7-1 for convenience. The new values of inductances will become L_1=L-0.2L and L_2=L+0.2L where L=0.388nH is the original inductance of the transformer windings in case 2. The expected value of phase noise obtained at each output is calculated below using Rael's phase noise expressions:

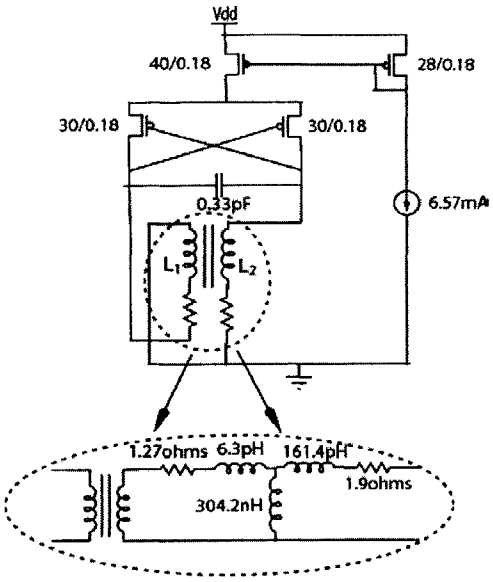

Figure 7-1: Transformer-based oscillator with mismatch in the inductance of the transformer windings

$L_1 = 0.8L = 310.4pH;\ L_2 = 1.2L = 465.6pH$
$R_1 = 0.8R = 1.268\Omega;\ R_2 = 1.2R = 1.902\Omega$

For inductor L_1

$R_P = Q^2 R_1 = 362.2\Omega;\ V_0 = I_{BIAS} * R_P = 6.57mA * 362.2 = 2.38V$
Phase noise, $L(\Delta f) = 1.18 * 10^{-15} \Rightarrow -149.3\,dBc/Hz$

Similarly, for inductor L_2

$R_P = Q^2 R_1 = 243.2\Omega;\ V_0 = I_{BIAS} * R_P = 6.57mA * 243.2 = 1.6V$
Phase noise, $L(\Delta f) = 1.53 * 10^{-15} \Rightarrow -148.2\,dBc/Hz$

Note that the above calculations assume that the Q of the transformer windings remains the same even though there is a mismatch in the value of their inductances. This assumption was made because small changes in the inductance of the transformer windings due to small variations in geometry will not cause significant changes in Q. The amplitude of the two differential output signals will no longer be equal because of the difference in the equivalent resistance of the two LC tanks. This arises from the fact that if

two inductors have approximately the same Q but different inductances, then they must have different series resistances as well.

The phase noise at the output with the higher signal amplitude increased by 0.5dB while that of the other output decreased by the same margin. Since this change in the phase noise is small, it can be concluded that a 20% mismatch in the inductance of the transformer windings does not have any significant effect on the phase noise of the oscillator.

A number of simulations were done in SpectreRF to verify the conclusions obtained from the analysis above. The transient response of the oscillator in Figure 7-1 with a 20% mismatch in the inductance of the transformer windings is shown in Figure 7-2:

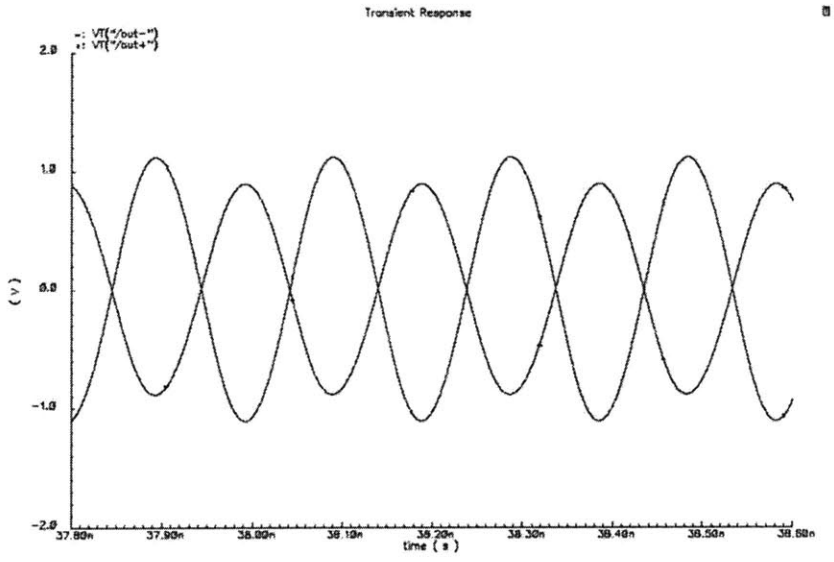

Figure 7-2: Transient response of LC oscillator with 20% mismatch between windings

The waveforms of the transient response shown in Figure 7-2 confirm that the signals obtained from the two output nodes of the oscillator are no longer equal. The amplitude of the output signal has changed from 2V p-p to 2.22V p-p and 1.77V p-p. There is a difference of about 7% from the simulated and calculated values. The center frequency

frequency of this oscillator is the same as that of a transformer-based oscillator shown in Figure 5-4 whose inductance is equal to the average of the mismatched inductances. Thus, because the two mismatched windings of the transformer have inductances of L-0.2L and L+0.2L where L is the inductance in the original transformer-based resonator in Figure 5-4, the average of these inductances is L, and the same center frequency of 5GHz was obtained. More importantly, the phase noise obtained from the SpectreRF simulation was -152.4dBc/Hz at 20MHz offset. When this is compared to the phase noise of -152.6dBc/Hz obtained for the original transformer-based resonator without mismatch (Figure 5-4), the conclusion that the mismatch in inductance values does not significantly affect the phase noise of the LC oscillator is confirmed.

It is worth mentioning that the results in this section are valid over all process and temperature variations. This is an obvious fact because these variations will affect each LC oscillator topology in exactly the same manner.

7.3 Summary

In this chapter, the effects of a mismatch in the inductances of the transformer windings were investigated. The results from both hand calculations and SpectreRF simulations indicated that the change in phase noise introduced by this mismatch was too small to be a serious issue. This analysis was done for a mismatch of 20% which is large for the well controlled silicon VLSI process currently available. This leads to the conclusion that mismatch in the inductances of the transformer windings will not be a serious issue in a practical transformer-based LC oscillator. The next chapter will conclude this thesis highlighting the major contributions achieved.

Chapter 8
Conclusion

This thesis has investigated an important approach or technique which can be used to increase the Q-factor of the resonator in an integrated LC oscillator and thus reduce the phase noise generated by these circuits. In particular, the advantage of using a transformer-coupled resonator instead of the standard inductor-based resonator in an oscillator has been shown to improve the Q-factor of the resonator by a factor equal to (1+k) where k is the coupling coefficient of the integrated transformer. For a typical coupling coefficient of k=0.8, the Q-factor of the resonator is increased by a factor of 1.8. It was shown that applying Leeson's phase noise formula, a reduction of 5.1dB in the phase noise of the oscillator's output when compared to a standard oscillator with identical design specifications is expected. Extensive SpectreRF simulations of the standard inductor-based (case 1) and transformer-coupled (case 2) oscillator verified this fact.

An alternative transformer-based architecture that is somewhat simpler than that used in [5] was proposed. This architecture was discussed in chapter 5 and eliminates the need for an extra varactor in a "floating" RLC which was used in [5]. An obvious advantage of using the proposed architecture proposed that the problems introduced by the inevitable mismatch in the varactors in [5] will not be an issue. This is because the proposed transformer-coupled resonator requires the use of just one varactor. Although it can be argued that the problems associated with any mismatch in the varactors can be resolved by using different bias voltages, a bank of fixed capacitors (Section 2.3.2), or

other techniques, it is simpler to use a transformer-coupled resonator that has single varactor as described in chapter 5.

In the analysis shown in Appendix A, an important discrepancy or inconsistency between the above mentioned results and theoretical analysis was revealed. This fact specifically applies to the transformer-based oscillator similar to that presented by Straayer et al in [5] and [12]. This design has a passive LC tank that is electrically isolated from the rest of the circuit in addition to the primary tank which is connected to the cross-coupled transistors and is responsible for the generation of the output signal. The inconsistency arises from the fact that a theoretical analysis indicates that the Q of the tank will not increase by a factor of $(1+k)$ but by $\frac{(1+k)}{(1+k^2)}$ because the main primary tank is loaded by the resistance reflected from the secondary "floating" passive tank. The interesting fact is the amplitude of oscillation from the SpectreRF simulation seems to support this assertion but the phase noise obtained from the same simulation appears to support the assertion that the Q-factor of the resonator increases by the factor $(1+k)$.

Although a suitable or acceptable explanation of this discrepancy was not provided in this thesis, the fact that the phase noise of an oscillator is reduced by using a transformer-coupled resonator was demonstrated. The author was able to show that a discrepancy between theory and simulation does exist and could be resolved in future research work.

A tradeoff between the requirements for high coupling coefficients (k) and high quality factors (Q) was discussed. The k vs. Q tradeoff is an important factor to take into consideration in the design of integrated transformers for high speed applications. This

issue is further accentuated by the relatively small values of inductances and capacitances required for multi-GHz applications.

Appendix A

An Alternative Transformer-Based Oscillator Topology

This appendix discusses Straayer's resonator topology which is presented in [5] and [12]. This topology is somewhat more complicated than case 3 in the previous chapter because it achieves the increase in Q by means of two separate LC tanks employing two varactors. Issues involving the matching of the two varactors and LC tanks are bound to arise with this resonator architecture.

The analysis will be conducted by means of two alternative methods. The first method will use the same simplifications employed in the analysis of the oscillator in case 2 discussed in Chapter 5. It should be noted that this analysis leads to conclusions which are inconsistent with the results obtained from SpectreRF simulations of the oscillator in case 3 shown in Figure A-1 below. An attempt will be made to account for this inconsistency. This analysis is included here for completeness and to show how a method of analysis which applies to a particular resonator topology may not apply to another.

The second method of analysis is based on the work in [12]. The discrepancy between the result of this second method of analysis and SpectreRF simulations will also be discussed.

A.1 Case 2: LC Oscillator with Transformer-Based Resonator which includes a passive secondary LC tank.

The transformer-based oscillator shown in Figure A-1 is similar to the oscillator discussed in Straayer et al [5]. While the design in [5] is complementary because it uses both NMOS and PMOS devices, the oscillator in Figure A-1 uses only PMOS devices to reduce the device noise introduced by these active devices. The oscillators in Figure A-1 and [5] are similar because they both have a secondary tank that is completely passive. In other words, one of the windings of the transformer used in the resonator is not connected to the active devices but left floating. The electrical isolation of this winding from the rest of the circuit is an obvious contrast to the topology considered in Section 5.3 which had both windings of the transformer connected to the differential pair PMOS transistors. This fact will be used in the analysis which follows.

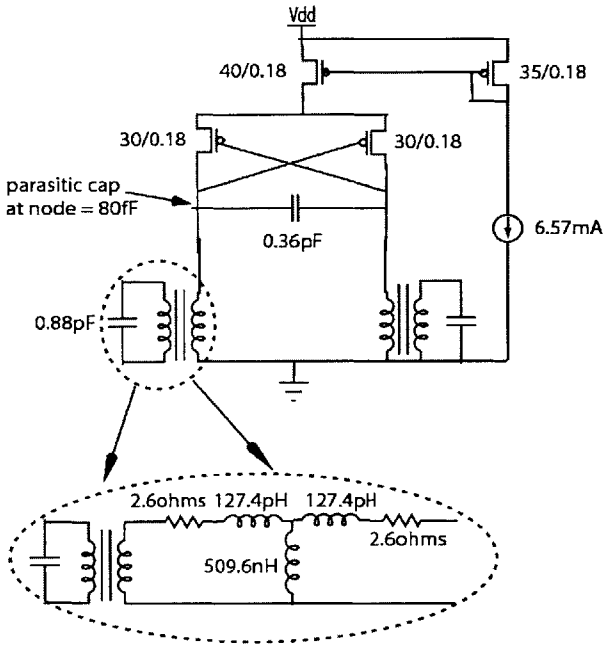

Figure A-1: Transformer-based LC VCO with passive secondary LC tank.

A.1.1 Calculation of the Effective Q of the resonator

Consider the simplified model of the transformer-based resonator in Figure A-2.

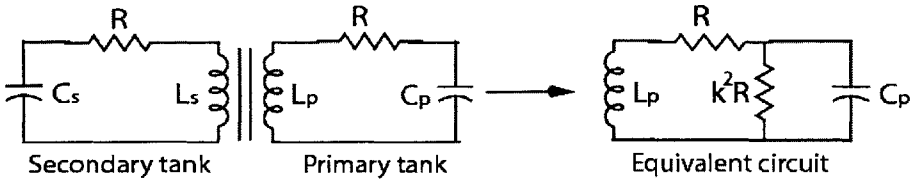

Figure A-2: Equivalent circuit of transformer-based resonator

When the secondary tank is at resonance, the impedance due to the capacitance, C_s, and inductance, L_s, will cancel out. Thus, only the resistance, R, is reflected into the primary tank as shown in the equivalent circuit of Figure A-2b. From this equivalent circuit, the impedance in series with the inductor is given by

$$R+\left(k^2R\left\|\frac{-j}{\omega C_P}\right.\right)=\frac{\left(1+k^2\right)R+\omega^2k^4R^3C_P^2-j\omega k^3R^2C_P}{k^2\omega^2R^2C_P^2} \tag{A.1}$$

For the values of R, C_P and L_P which occur in practical oscillators, $\omega^2k^4R^2C_P^2$, $\omega^2k^2R^3C_P^2$ and $\omega k^3R^2C_P$ are relatively small and can be ignored in (A.1). Thus, the effective impedance in series with the inductor is approximately $\left(1+k^2\right)R$. In essence, the primary tank reduces to an inductor, L_P+M in series with a resistance, $\left(1+k^2\right)R$. The Q-factor of this structure is calculated below:

If $L_P=L_S=L$ and $C_P=C_S=C$ then $M=k\sqrt{L_PL_S}=kL$

$$Q_{case2}=\frac{\omega_0L_{eff}}{R_{eff}}=\frac{\omega_0\left(1+k\right)L}{\left(1+k^2\right)R}=\frac{\left(1+k\right)}{\left(1+k^2\right)}Q_{case1}$$

where $Q_{case1}=\dfrac{\omega_0L}{R}$ (from Chapter 5)

The coupling coefficient, k = 0.8 remains the same because the same transformer which was used in the oscillator topology in case 2 will be used here. Given that Q_{case1}=7.69. the quality factor of the resonator is calculated as,

$$Q_{case2} = \frac{(1+0.8)}{(1+0.8^2)} * 7.69 = 8.44$$

This quality factor is lower than the expected value of 13.85 which was obtained in case 2.

A.1.2 Oscillator Design

Once again it is desirable to design this oscillator with exactly the same operating point and specification as the two previous topologies to facilitate easy comparison. Using a methodology similar to that used for the design in case 2, an inductor size was selected to set the equivalent parallel resistance to a value that makes the amplitude of oscillation 2V when the tail bias current is 6.57mA. The value of capacitance is chosen to set the resonant frequency to 5GHz.

$If\ V_{swing} = 2V\ and\ I_{BIAS} = 6.57mA$ (same as case 1 and case 2)

$Then, R_{eff} = \frac{V_{swing}}{I_{BIAS}} = 304\Omega$

$Also, R_p = R_{eff} = R_{L,eff} Q_{case2}^2 = R_{L,eff} * 8.44^2 \Rightarrow R_{L,eff} = 4.268\Omega$

where $R_{L,eff}$ is the effective series resistance in the tank.

$R_{L,eff} = (1+k^2) R_{L,case2} \Rightarrow R_{L,case2} = 2.6\Omega$

Since for and inductor, inductance, L, scales linearly with series resistance, R,

$$L_{case2} = L_{case1}\frac{R_{L,case2}}{R_{L,case1}} = 1.259nH * \frac{2.6}{5.142} = 0.637nH$$

$$L_{eff} = (1+k)L_{case2} = 1.15nH$$

$$from\ f_0 = \frac{1}{2\pi\sqrt{L_{eff}C}} = 5GHz, C = 0.881pF$$

The active device network which was used in case 1 will also be used for the oscillator topology in case 2.

A.1.3 Phase Noise Calculation

The parameters calculated above are now used to calculate the phase noise in the output of the oscillator using Rael's phase noise expressions as was done for case 3 in Section 5.3.

Resonator Noise

$$\mathrm{L}(\Delta f_0 = 20MHz) = N_1 N_2 \frac{kTR_{eff}}{V_0^2}\left(\frac{f_0}{2Q\Delta f_0}\right)^2 = 5.52*10^{-16}$$

where $N_1 = 2; N_2 = 4$

$$V_0 = V_{SWING} = 2V$$

Tail Current Noise

$$\mathrm{L}(\Delta f_0 = 20MHz) = \frac{32}{9}\gamma g_{m,TAIL} R_{eff}\frac{kTR_{eff}}{V_0^2}\left(\frac{f_0}{2Q\Delta f_0}\right)^2 = 1.23*10^{-15}$$

$$where\ \gamma = noise\ factor = 2.5; \mathrm{g_{m,TAIL}} = g_{PMOS} = 6.58mS$$

Differential Pair Noise

$$\mathrm{L}(\Delta f_0 = 20MHz) = \frac{32\gamma I_{BIAS} R}{\pi V_0}\frac{kTR}{V_0^2}\left(\frac{f_0}{2Q\Delta f_0}\right)^2 = 1.76*10^{-15}$$

$$\mathrm{L_{TOTAL}}(\Delta f_0 = 20MHz) = 5.22*10^{-16} + 1.23*10^{-15} + 1.76*10^{-15}$$
$$= 3.51*10^{-15}$$

$$\text{Phase noise} = 10\log(\mathrm{L_{TOTAL}}(\Delta f_0 = 20MHz)) = -144.6\,dBc/Hz$$

The above results were checked by simulating the circuit of Figure A-1 in SpectreRF. The phase noise obtained from the simulation was -152.2dBc/Hz at 20MHz offset with the center frequency = 5.06GHz.

A.2 Analysis of results

The results obtained for case 1 and case 3 are compared in the table below:

	Phase Noise (dBc/Hz) @ 20MHz offset with a 5GHz center frequency		
	Case 3	Case 2	
		Hand calculations	Matlab analysis
Calculated	-148.8	-144.6	-148.9
Simulated (SpectreRF)	-152.6	-152.2	-152.2
Relative Difference (dB)	3.8	7.6	3.3

Table A-1: Summary of results obtained in case 2 and case 3 topologies of the LC oscillator.

The results presented in the table above show that the hand calculated value of phase noise for case 3 is significantly larger than that of case 2. This is because of the difference in the Q-factors of the resonators in the two topologies. But SpectreRF simulations show a close agreement between the phase noise of the two topologies. Furthermore, the phase noise obtained from the SpectreRF simulations of case 2 is significantly smaller than the value calculated using the Rael's phase noise expressions. These discrepancies between the phase noise derived from hand analysis and that obtained from SpectreRF simulations presents an obvious problem. Although the magnitude of the phase noise obtained from SpectreRF simulations is what would be expected if the Q of the tank is increased by a factor of $(1+k)=1.8$ (as in case 3 of Chapter 5), the amplitude

of the output signal is what would be expected if the Q of the tank is increased by a smaller factor of $\frac{(1+k)}{(1+k^2)}$=1.1. The oscillator in case 2 was designed to have an output signal amplitude of 2V assuming that the Q was increased by the smaller factor of 1.1. This assumption was verified from the amplitude obtained when the oscillator was simulated in SpectreRF. In contrast, the phase noise obtained from the same SpectreRF simulation is significantly smaller than would be expected for this lower value of Q. If the phase noise from the SpectreRF simulation of case 2 is compared to that obtained in case 3, it would appear the higher value of Q = 13.85 must be correct to explain the improved phase noise performance. Thus, these results present a clear contradiction.

An ac simulation of the transformer-based resonator was done in SpectreRF to calculate its quality factor. The circuit in Figure A-3 below was used in the analysis.

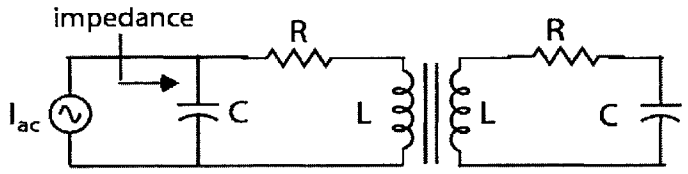

Figure A-3: Test circuit used to determine the Q of the transformer-based resonator.

Figure A-4: Impedance plot of transformer-based resonator

The impedance plot in Figure A-4 was obtained by taking the ratio of the voltage to the current at the terminals of the ac current source, I_{ac}. The Q-factor was calculated from this impedance plot using the 3-db bandwidth definition.

$$Q = \frac{\text{center frequency}}{\text{3dB bandwidth}} = \frac{5*10^9}{3.58*10^8} = 13.9$$

When the phase noise of the oscillator was recalculated using the higher Q-factor of 13.9, the value obtained was -148.9 dBc/Hz at a 20MHz offset from the center frequency of 5GHz. This value is close to that obtained from SpectreRF simulations.

This simulation does confirm the fact that the Q of the transformer-based resonator is actually increased by the factor of (1+k). The problem with this conclusion is the fact that the output amplitude of oscillation is lower than would be expected for this larger value of Q. This assertion is clarified by calculating the expected output signal amplitude using the higher Q-factor of 13.85.

$$V_{swing} = I_{BIAS} * R_P$$
$$where\ I_{BIAS} = tail\ bias\ current$$
$$and\ R_P = \text{equivalent parallel resistance}$$
$$R_P = R_{L,case3} * Q^2 = 2.6*13.85^2 = 498.7\Omega$$
$$\Rightarrow V_{swing} = 6.57mA*498.7\Omega = 3.28V$$

This calculated value of the output swing is greater than the value of 2V obtained from the SpectreRF simulation.

The oscillator in Figure A-1 was re-simulated in SpectreRF using the same transformer specifications as the oscillator in case 3 of Section 5.3 except that the secondary or passive tank was made lossless so that no resistance is reflected into the primary tank connected to the active device network. Thus, the inductance and resistance of the primary and were 0.388nH and 1.585Ω and the corresponding values for the secondary tank

were 0.388nH and 0.001Ω (≈ 0) respectively. The results of the simulation showed that the amplitude of oscillation was 2V which is the expected magnitude when the Q-factor of the transformer winding is increased by a factor of (1+k) as in case 3. This result indicates that the now "ideal" passive "floating" LC tank no longer loads the primary tank. Thus, an apparent conclusion which can be drawn from this result is that the passive "floating" LC tank loads the primary tank and thus reduces the Q-factor of the resonator. This further shows the obvious discrepancy between hand analysis and intuition versus SpectreRF simulations.

It appears a more subtle reason needs to be proposed to explain this apparent discrepancy. One thought is the fact that the previous analysis approximates the transformer network as a second order system. This is essentially not accurate because the system is fourth order owing to the presence of four storage elements. An analytical proof of the fact that the transformer-based resonator's Q increases by the factor (1+k) is shown in [12]. The key conclusions from the electrical analysis done in that paper are presented below:

Consider the simplified model of the transformer-based resonator network in Figure A-5:

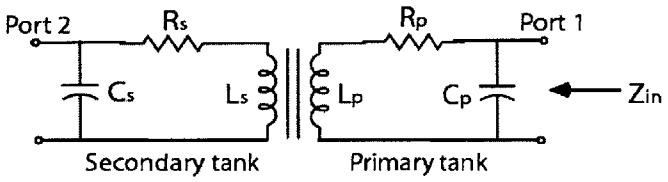

Figure A-5: simplified model of transformer-based resonator tank

Writing KVL for the primary and secondary tanks, the following expressions are obtained:

$V_1 = j\omega L_p I_1 + R_p I_1 + j\omega M I_2$

$V_2 = j\omega L_s I_2 + R_s I_2 + j\omega M I_1$

where V_1, V_2 are the voltages across C_p, C_s and I_1, I_2 are the currents in the primary and secondary tank respectively.

Using simple circuit analysis, the expression for the impedance of the circuit looking into port 1, Z_{in} is given by,

$$Z_{in} = \frac{\omega^2\left(M^2 - L_p L_s\right) + \frac{L_p}{C_s} + R_p R_s + j\left(\omega L_p R_s + \omega L_s R_p - \frac{R_p}{\omega C_s}\right)}{R_s - \omega C_p\left(\omega L_p R_s + \omega L_s R_p - \frac{R_p}{\omega C_s}\right) + j\left[\omega C_p\left(\omega^2\left(M^2 - L_p L_s\right) + \frac{L_p}{C_s} + R_p R_s\right) + \omega L_s - \frac{1}{\omega C_s}\right]}$$

At resonance, the imaginary component of the impedance, $Z_{in} = 0$. Furthermore, for the values of resistance, capacitance, and inductance encountered in practical oscillators, the resistances R_p, R_s have no effect on the resonant frequency and can be ignored. Imposing this constraint on the equation above, the resonant frequency becomes:

$$\omega_1^2 = \frac{\left(L_p C_p + L_s C_s\right) + \sqrt{\left(L_p C_p + L_s C_s\right)^2 + 4C_p C_s\left(M^2 - L_p L_s\right)}}{2C_p C_s\left(M^2 - L_p L_s\right)}$$

$$\omega_2^2 = \frac{\left(L_p C_p + L_s C_s\right) - \sqrt{\left(L_p C_p + L_s C_s\right)^2 + 4C_p C_s\left(M^2 - L_p L_s\right)}}{2C_p C_s\left(M^2 - L_p L_s\right)}$$

If the transformer-based resonator is symmetric, $C_p = C_s = C$ and $R_p = R_s = R$. Thus, the expression for the resonant frequencies simplify to,

$$\omega_1^2 = \frac{1}{(L+M)C} \text{ and } \omega_2^2 = \frac{1}{(L-M)C}$$

Substituting the values of ω_1^2 and ω_2^2 into the expression for Z_{in} above,

$$Z_{in,1} \approx \frac{L+M}{2RC} \text{ and } Z_{in,2} \approx \frac{L-M}{2RC}$$

Finally, the Q of the transformer-based resonator is calculated based on the phase slope formula, $Q = \frac{\omega}{2}\frac{\partial\theta}{\partial\omega}$

$$\theta = \tan^{-1}\frac{\mathrm{Im}(Z_{in})}{\mathrm{Re}(Z_{in})}$$

$$\left.\frac{\partial\theta}{\partial\omega}\right|_{\omega=\frac{1}{\sqrt{(L+M)C}}} = \frac{2(L+M)+R^3C}{R+\frac{R^3C}{2L}}$$

$$\Rightarrow Q\Big|_{\omega=\omega_1=\frac{1}{\sqrt{(L+M)C}}} = \frac{\omega_1(L+M)}{R}$$

$$but\ M = kL$$

$$\therefore Q\Big|_{\omega=\omega_1=\frac{1}{\sqrt{(L+M)C}}} = \frac{(1+k)\omega_1 L}{R}$$

Thus, the calculation above proves that using a transformer-based resonator increases the Q of the tank by a factor of (1+k). This analysis is verified using the bode plot of the equivalent impedance of the transformer-based resonator shown in Figure A-6. The Q of the tank is calculated using the 3-db bandwidth definition,

$$Q = \frac{\text{center frequency}}{\text{3 - dB bandwidth}} = \frac{\omega_0}{\Delta\omega} = \frac{2\pi(5*10^{9})}{(5.19-4.83)*10^{9}} = 13.88$$

Once again, the phase noise can be recalculated using the same procedure as described in Section A.1.3. The phase noise obtained was -148.9 dBc/Hz at a 20MHz offset from the center frequency of 5GHz. This value agrees with the results from SpectreRF simulations of the oscillator in Figure A-1.

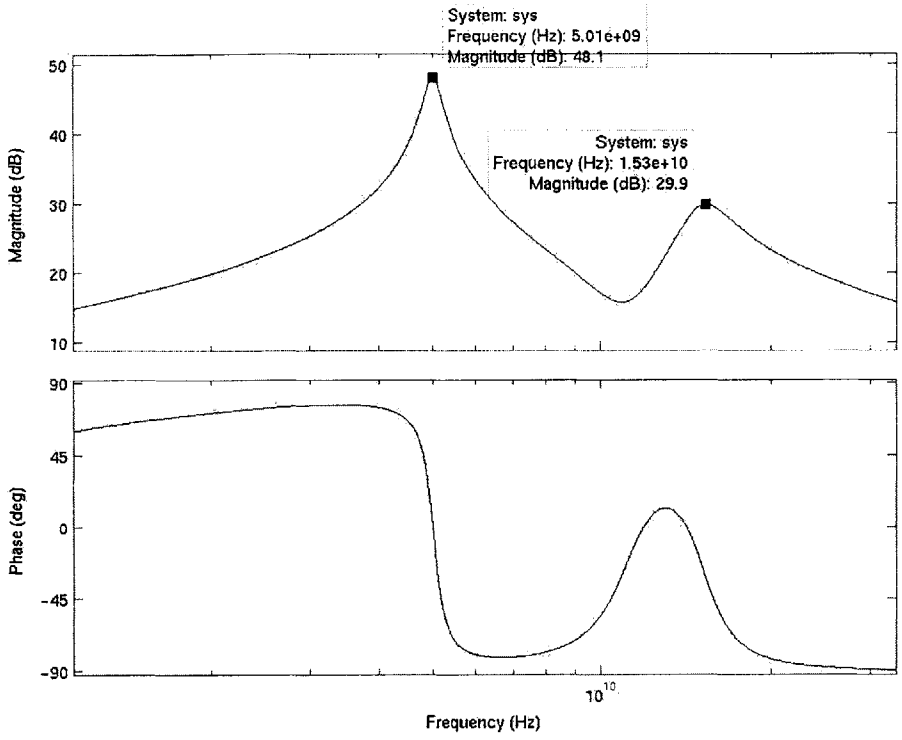

Figure A-6: Bode diagram of the equivalent impedance of the transformer-based resonator.

Unfortunately, this still does not explain the apparent discrepancy discussed earlier in this section. Although the above calculation proves that the Q-factor of the transformer-based oscillator is increased by a factor of (1+k), this does not agree with the results obtained from SpectreRF simulations. It appears that analyzing the current problem from an energy storage perspective may explain or eliminate this apparent discrepancy. This method of analysis could be the subject of future work.

Bibliography

[1] T.H. Lee, A. Hajimiri, "Oscillator Phase Noise: A Tutorial," *IEEE Journal of Solid-State Circuits,* vol. 35, March 2000, pp. 326-336.

[2] D.B. Leeson, "A simple model of feedback oscillator noise spectrum," in *Proc. IEEE,* vol. 54, February 1966, pp. 329-330.

[3] J.J. Rael, A.A. Abidi, "Physical Processes of Phase Noise in Differential LC Oscillators," *IEEE Custom Integrated Circuits Conference,* 2000.

[4] A. Hajimiri, T.H. Lee, "A General Theory of Phase Noise in Electrical Oscillators," *IEEE Journal of Sold-State Circuits,* vol 33, February 1998, pp. 179-194.

[5] M. Straayer, J. Cabanillas, G.M. Rebeiz, "A Low-Noise 1.7GHz CMOS VCO," *IEEE ISSCC Digest of Technical Papers,* vol 1, 2002, pp. 286-287.

[6] A. Hajimiri, T.H. Lee, "Design Issues in CMOS Differential Oscillators," *IEEE Journal of Solid-State Circuits,* vol. 34, May 1999, pp. 717-724.

[7] M. Danesh, J.R. Long, R.L. Hadaway, D.L. Harame, "A Q-factor Enhancement Technique for MMIC Inductors," *IEEE Radio Frequency Integrated Circuits (RFIC) Symposium,* June 1998, pp. 217-220.

[8] E. Hegazi, H. Sjoland, A.A. Abidi, "A Filtering Technique to Lower LC Oscillator Phase Noise," *IEEE Journal of Solid-State Circuits,* vol. 36, December 2001, pp. 1921-1930.

[9] A.M. Niknejad, R.G. Meyer, "Analysis, Design, and Optimization of Spiral Inductors and Transformers for SI RF IC's," *IEEE Journal of Solid-State Circuits,* vol 33, October 1998, pp. 1470-1481.

[10] J.R. Long, "Monolithic Transformers for Silicon RF IC Design," *IEEE Journal of Solid-State Circuits,* vol 35, No. 9, September 2000, pp. 1368-1382

[11] B. Razavi, "RF Microelectronics," *Prentice Hall,* 1998.

[12] Jose Cabanillas, Matt Straayer, Jose M. Lopez-Villegas and Gabriel M. Rebeiz, "A Transformer-Based Low Phase Noise CMOS Oscillator," *Submitted for publication in the IEEE Journal of Solid State Circuits, July 2003.*

[13] P.R. Gray, P.J. Hurst, S.H. Lewis, R.G. Meyer, "Analysis and Design of Analog Integrated Circuits", *John Wiley & Sons,* 2001.

[14] P. Andreani, "A 1.8 GHz Monolithic CMOS VCO tuned by an Inductive Varactor", *IEEE International Symposium on Circuits and Systems,* vol 4, May 2001, pp 714-717.

[15] M.H. Perrott, "High Speed Communication Circuits and Systems", *6.976 Lecture Notes, http://www-mtl.mit.edu/~perrott,* March 2003.

[16] A. Worapishet, S. Ninyawee, "Magnetically-Coupled Tunable Inductor for wide-band variable frequency oscillators", *IEEE International Symposium on Circuits and Systems,* vol 4, May 2001, pp 517-520.

[17] S.S. Mohan, M.M. Hershenson, S.P. Boyd, T.H. Lee, "Simple Accurate Expressions for Planar Spiral Inductances", *IEEE Journal of Solid-State Circuits,* vol 34, October 1999, pp 1419-1424.

[18] A. Hajimiri, S. Limotyrakis, T.H. Lee, "Jitter and Phase Noise in Ring Oscillators," *IEEE Journal of Solid-State Circuits,* vol. 34, no. 6, June 1999, pp 790-804.

[19] H. Darabi, A.A. Abidi, "Noise in RF-CMOS Mixers: A Simple Physical Model," *IEEE Transactions on Solid-State Circuits,* vol. 35, no. 1, January 2000, pp 15-25.

[20] C.P. Yue, C. Ryu, J. Lau, T.H. Lee, S.S. Wong, "A Physical Model for Planar Spiral Inductors on Silicon," *International Electron Devices Meeting,* 8-11 Dec. 1996, pp 155 -158

[21] K. A. Kouznetsov, R. G. Meyer, "Phase Noise in LC Oscillators," *IEEE Journal of Solid-State Circuits,* vol. 35, no. 8, August 2000, pp 1244-1248.

[22] K. Mayaram, D.O. Pederson, "Analysis of MOS Transformer-Coupled Oscillators," *IEEE Journal of Solid-State Circuits,* vol. sc-22, no. 6, December 1987.